Joint Estimation of Direction of Arrival with Unknown Mutual Coupling in Massive MIMO Networks and LTE Radio Resource Block Allocation Optimization in Maritime Channels

A thesis submitted to the
Graduate School of Natural and Applied Sciences

by

Amit KACHROO

in partial fulfillment for the
degree of Master of Science

in

Electronics and Computer Engineering

İSTANBUL
ŞEHİR
UNIVERSITY

This is to certify that we have read this thesis and that in our opinion it is fully adequate, in scope and quality, as a thesis for the degree of Master of Science in Electronics and Computer Engineering.

APPROVED BY:

Assist. Prof. Dr. Mehmet Kemal Özdemir ....
(Thesis Advisor)

Assoc. Prof. Dr. Serhan Yarkan ....

Assist. Prof. Dr. Hatice Tekiner-Mogulkoc ....

This is to confirm that this thesis complies with all the standards set by the Graduate School of Natural and Applied Sciences of İstanbul Şehir University:

DATE OF APPROVAL: 6 May 2017

SEAL/SIGNATURE:

Declaration of Authorship

I, Amit KACHROO, declare that this thesis titled, 'Joint Estimation of Direction of Arrival with Unknown Mutual Coupling in Massive MIMO Networks and LTE Radio Resource Block Allocation Optimization in Maritime Channels' and the work presented in it are my own. I confirm that:

- This work was done wholly or mainly while in candidature for a research degree at this University.

- Where any part of this thesis has previously been submitted for a degree or any other qualification at this University or any other institution, this has been clearly stated.

- Where I have consulted the published work of others, this is always clearly attributed.

- Where I have quoted from the work of others, the source is always given. With the exception of such quotations, this thesis is entirely my own work.

- I have acknowledged all main sources of help.

- Where the thesis is based on work done by myself jointly with others, I have made clear exactly what was done by others and what I have contributed myself.

Signed:

Date: 11 - May - 2017

"An equation means nothing to me unless it expresses a thought of God. "

Srinivasa Ramanujan

Joint Estimation of Direction of Arrival with Unknown Mutual Coupling in Massive MIMO Networks and LTE Radio Resource Block Allocation Optimization in Maritime Channels

Amit KACHROO

Abstract

The evolution of technology from one generation to other always brings a better user experiences in terms of high data rates and improved quality of service parameters like low latency. However, it also comes with its own challenges. The upcoming 5G technology is one of those technologies that is now moving from theory to practical implementation with prototypes being developed all around the world. Massive MIMO is the key enabler for such 5G networks and one of the concerns with massive MIMO is the mutual coupling effect that causes wrong direction of arrival (DoA) estimations that leads to low capacity issues. In this thesis, several optimization techniques related to estimations of DoA and unknown mutual coupling in antenna arrays are studied and an extended joint iterative optimization with reduced rank method is proposed in that cause considering massive MIMO networks. The backbone of the work is based on joint iterative method with reduced rank matrix optimization, quadratic programming (QP), compressed sensing and L_2 norms that are used to determine the DoAs and unknown mutual coupling with higher resolution capabilities. The proposed method is dynamic in nature and has very low complexity order giving it a big advantage over other methods. Furthermore, in absence of any 5G standards radio resource block allocation methods for LTE over sea are studied and a max-min optimization is proposed which is then compared with the previous resource allocation algorithms. The results of the proposed resource allocation method reflects the superiority of the algorithm in terms of fairness with variable load. In summary, this thesis shreds light into the application of convex optimization and linear algebra in wireless communication domain.

Keywords: Massive MIMO, ULA, UCA, MVDR, MUSIC, ESPRIT, DoA, Mutual Coupling, QP, convex optimization, JIO, LTE, 3-Ray Path loss Modelling, Max-min Integer Linear Programming, SINR, Fairness, Radio Resource Block Allocation

Masif MIMO Ağlarında Bilinmeyen Karşılıklı Etkileşimle Ortak Varış Yönü Tahmini ve Deniz Kanallarıda LTE Radyo Kaynak Bloğu Tahsis Optimizasyonu

Amit Kachroo

Öz

Teknoloji bir kuşaktan diğerine evrilirken, yüksek veri hızı ve düşük gecikme gibi hizmet kalitesini yükselten parametrelerle daha iyi bir kullanım deneyimi sunmaktadır. Fakat bu iyileşme, beraberinde bazı zorluklar getirmektedir. Yaklaşan 5G teknolojisi, şu an tüm dünyada teoriden pratik uygulamaya geçmekte olan ve prototipleri geliştirilen teknolojilerin başında yer almaktadır. Çoklu (Massive yada Masif) MIMO, 5G kablosuz ağlarının gerçeklendirilmesinde önemli bir safhayı oluşturmaktadır. Fakat masif MIMO'nun performansını önemli derecede etkilyen ve düşük kapasite sorunlarına sebep olan etkenler mevcuttur. Bunların başında varış açısı yönünün (DoA) hatalı olarak kestirimine sebep olan karşılıklı bağlaşım etkisidir. Bu tezde, DoA ve anten dizilişlerindeki bilinmeyen karşılıklı bağlaşım etkilerinin tahmini için birçok optimizasyon tekniği incelenmiş ve masif MIMO ağları için indirgenmiş rank metoduyla genişletilmiş ortak döngüsel optimizasyon önerilmiştir. Bu çalışmanın temel omurgasını oluşturan yaklaşım indirgenmiş rank metoduyla ortak döngüsel optimizasyonu, kuadratik programlama (QP), sıkıştırılmış algılama, ve DoA ve bilinmeyen karşılıklı bağlaşımın saptanmasında kullanılan ve de yüksek çözünürlülük kapasitesine sahip L2 normu oluşturmaktadır. Önerilen yöntemin temelde dinamik bir yapıya sahip olması ve diğer yöntemlere kıyasla çok düşük karmaşıklık derecesi içermesi en büyük avantajlarındandır. Ayrıca, 5G standartlarının netleşmemesinden dolayısıyla LTE için mevcut deniz aşırı radyo kaynak bloğu tahsis yöntemleri incelenmiş ve mevcut kaynak tahsis algoritmalarıyla kıyaslanarak max-min optimizasyonu önerilmiştir. Önerilen tahsis yönteminin sonuçları, algoritmanın değişebilen yük ile daha adil kaynak tahsisi yaptığını yansıtmaktadır. Özetle, bu tez dışbükey optimizasyon ve doğrusal cebirin kablosuz iletişim uygulamalarındaki önemini göstermektedir.

Anahtar Sözcükler: Optimizasyon, LTE, 3-Ray Elektromanyetik Yol Kaybı, Max-min Tamsayı Linear Programlama, SINR, Radyo Kaynak Bloğu Tahsisi

I would like to dedicate this work to my parents and to my late grandmother, Mrs. Durga Devi Kachroo, who always stood behind me through thin and thick times and kept believing in me.

Acknowledgments

The graduate study at Istanbul Sehir University has been very momentous and exciting. I would like to express my deep gratitude to many people, who have helped me a lot and made these years wonderful.

Moreover, I would also like to put on record special thanks to Professor Serhan Yarkan, Professor Hatice Tekiner-Mogulkoc, Ali Uzun and Ihsan Albittar for their help and support through out my time at Istanbul Sehir University. I will always cherish the memories we had together.

Last but not the least, I would like to express my deepest and sincerest appreciation to my parents, sister and friends back in India and South Korea for their patience, encouragement, love and providing me constant support throughout my life. They have been inspiring to me at every moment.

Contents

List of Figures

List of Tables

Abbreviations

AWGN	Additional white gaussian noise
SoI	Signal of interest
NSoI	Non Signal of interest
MIMO	Multiple input multiple output
DoA	Direction of arrival
MVDR	Minimum variance distortionless response
MUSIC	Multiple signal classification algorithm
ESPRIT	Estimation of signal parameters via rotational invariance technique
JIO	Joint iterative optimization
LTE	Long term evolution
5G	Fifth generation mobile networks
MCS	Modulation and coding scheme
SNR	Signal to noise ratio
SINR	Signal to interference noise ratio
ULA	Uniform linear array
UCA	Uniform circular array
ML	Maximum likelihood
QP	Quadratic programming
RB	Resource block
TDMA	Time domain multiple access
CDMA	Code division multiple access
OFDMA	Orthogonal frequency division multiplication access
FDMA	Frequency division multiplication access
CSI	Channel state information

Physical Constants

Speed of Light $\quad c \quad = \quad 2.997\ 924\ 58 \times 10^8$ ms^{-S} (exact)

Symbols

Symbol	Name	Unit
d	distance	m
P	power	W (Js^{-1})
ω	angular frequency	radian/s
θ	elevation angle	degree (°)
ϕ	azimuth angle	degree (°)
v	voltage	volts

Chapter 1

Introduction to 5G Networks

1.1 Evolution of Cellular Technologies

The vast advancement in mobile wireless communication since last few decades has been path breaking. Each generation of wireless technology came up with its own technology standards that were unique and different than the previous one's. The first generation (1G) mobile wireless communication network was meant only for voice calls (analog communication) and was based on frequency division multiple access (FDMA) technology. On the other hand, second generation (2G) was a digital technology and supported text messaging with packet rates ranging from 10 Kbps to 64 Kbps. It relied on time domain multiple access (TDMA). Moving forward, the third generation (3G) mobile technology revolutionized the data speed and started supporting multimedia platform. This was due to code division multiple access (CDMA) technology with data rates ranging from 64 Kbps to 2 Mbps. Approximately, after a decade came the fourth generation (4G) technology which brought the mobile internet broadband concept into picture with maximum speeds going up to 100 Mbps. This was due to orthogonal frequency division multiplication access (OFDMA) technology. Now, the latest much talked 5G or 5th generation mobile technology in which not just internet broadband but also networked society is being considered is supposed to deliver data speeds from 1 Gbps to 10 Gbps. Figure 1.1 shows the evolution of the mobile wireless technology from 1G to 5G. In next section, massive MIMO, the key enabler behind the 5G technology is discussed in brief.
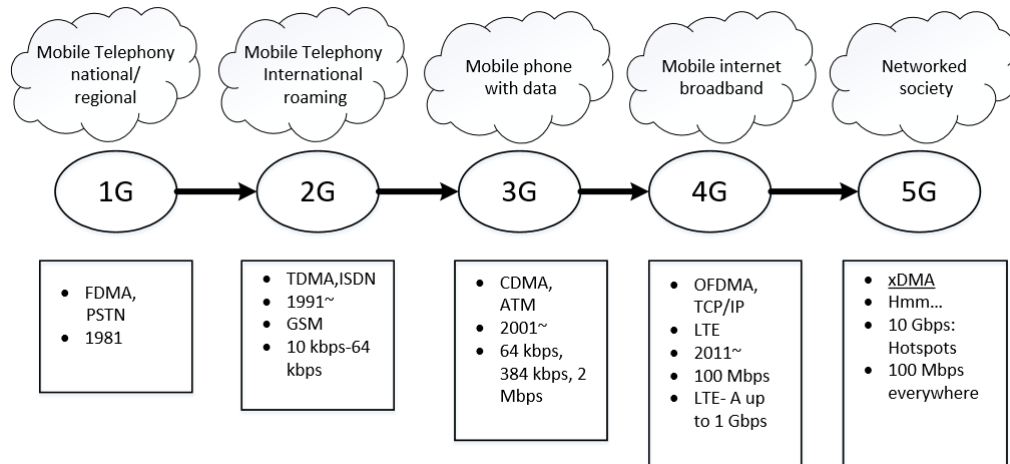
FIGURE 1.1: Evolution of cellular technologies from 1G to 5G

1.2 Massive MIMO for 5G

Massive MIMO holds an immense prospects for 5G wireless research and in next-generation wireless networks as it promises significant gains that offer the ability to accommodate many users at higher data rates with better reliability while consuming less power. This much talked 5G technology that gives unprecedented improvements in network throughput and capacity, enhancements in spectral efficiency, reduced end-to-end latency, and increased reliability is now being implemented practically. The performance improvement in 5G as is 20 times more than 4G which means 20Gbps as compared to 1Gbps.
In a nutshell, massive MIMO has many (hundreds) of antennas that serve in parallel tens of terminals. Figure 1.2 shows the typical 5G massive MIMO cell as compared to that of 4G MIMO cell, where the former is loaded with many more antennas at base station. Extra antennas brings huge improvements in throughput and radiated energy efficiency in the network. The other advantages of massive MIMO are the low cost low-power components, simple MAC layer, and robustness against jamming [1]. Many deployment configuration with massive MIMO are envisioned as shown in Figure 1.3, which are cylindrical, rectangular, linear or distributed.

With every new technology comes it's limitation or challenge set. In massive MIMO, apart from pilot contamination, hardware impairments, channel characterizations, the capacity impairments is a very challenging task. The main reason for capacity impairment is the channel correlation that affects the performance in a big way. In general, if the channel correlation is greater then the channel capacity goes smaller. The main

reasons for channel correlation are spatial correlation and antenna mutual coupling. In this work, the focus is especially laid on mutual coupling part.
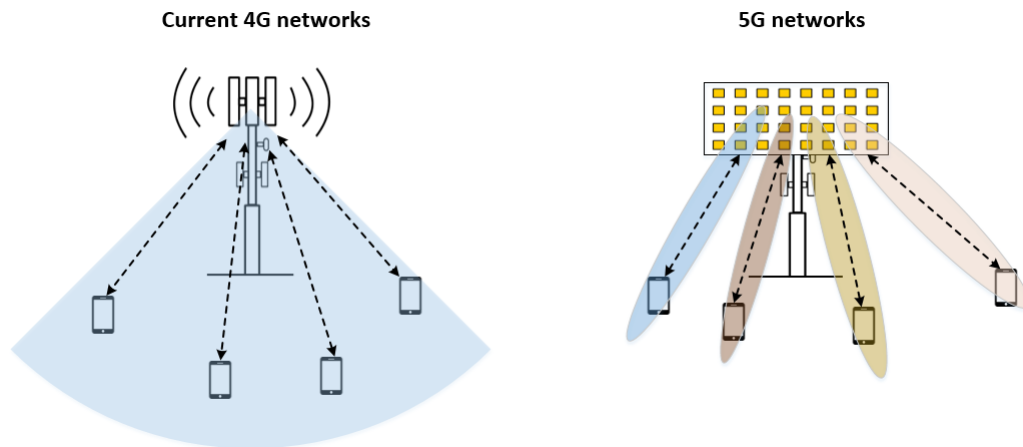
FIGURE 1.2: Multiantenna technology : 4G MIMO to 5G massive MIMO
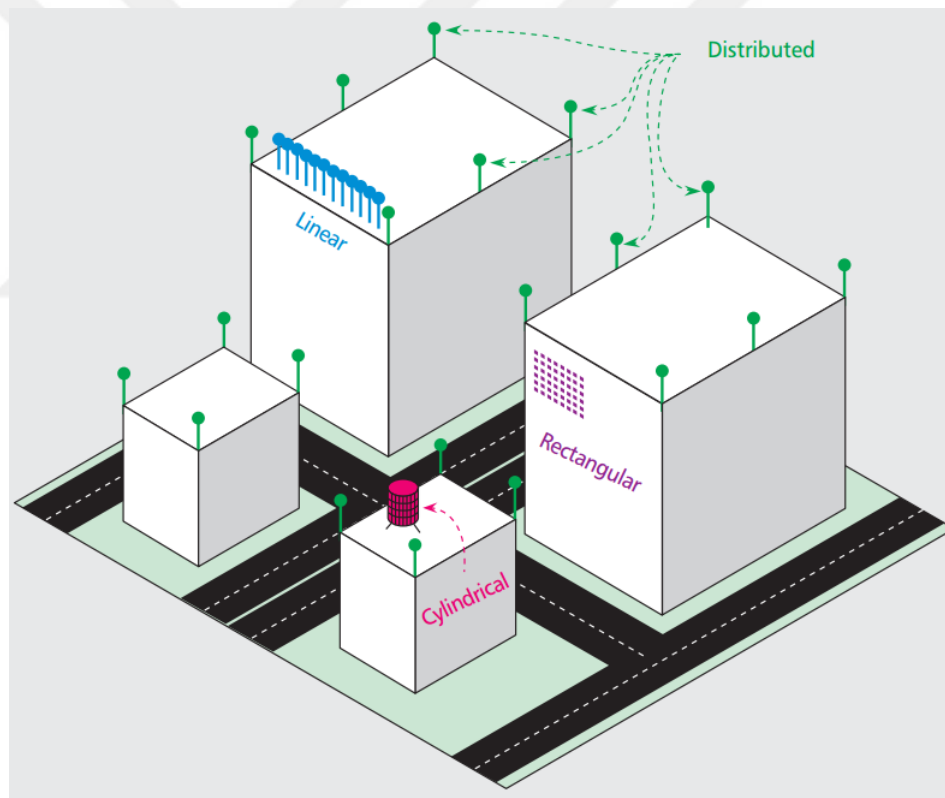
FIGURE 1.3: Massive MIMO antenna configurations [1]

1.3 Motivation Behind the Work

The main motivation behind this thesis work is not just to understand the estimation of DoAs but to consider mutual coupling while estimating DoAs in massive MIMO networks

for 5G. This can be accomplished only by using joint iterative optimization methods. To our best knowledge, this work is the first to consider joint estimation of DoAs and unknown mutual coupling in massive MIMO networks for 5G. The results thus obtained from the proposed method for DoA estimation with unknown mutual coupling show a big reduction in complexity as compared to other DoA estimation methods, which is discussed in later chapters. Also, the proposed method can be viewed as an extension of JIO algorithm [3] with a difference that it estimates the DoAs with unknown mutual coupling. In addition to that, post optimization techniques for better DoA resolution are discussed and proposed thereafter. The proposed post optimization methods have superiority over other methods in that they are dynamic with excellent resolution in nature. Furthermore, in absence of 5G standards, a max-min radio block resource allocation method is proposed for LTE in marine channels. The results showed better fairness as compared to other classical methods of radio resource block allocation. In next chapters, all the assumptions and details regarding joint DoA estimation with unknown mutual coupling and radio resource block allocation for LTE over sea will be discussed in detail. Also, proposed methods, comparisons and results thus obtained will be discussed with it.

Chapter 2

DoA Estimation by Classical Methods in Massive MIMO

2.1   Introduction

Array signal processing has many applications that include sonar, radar and wireless communication networks [4] and one of the major aim of array processing is to estimate DoAs in wireless networks. The action starts when an electromagnetic wave impinges upon an array of antenna's and the associated signal's are processed to extract DoAs with other intelligible information. DoA extraction methods are used to design and adapt the directivity of array antennas in a better way so as to align the beam towards signal of interest (SoI) and reject non signal of interest (NSoI) or interference. This can be visualized from the Figure 2.1. By doing so, a high SNR is guaranteed which in turn reflects in high capacity for the network.

Broadly, the DoA estimation methods are divided into three main domains: classical, sub space and maximum likelihood methods [5, 6]. Among these algorithms, the maximum likelihood (ML) method offers high performance with increased computational cost. On the other hand, subspace methods have better performance and have less cost for computation. On the contrary, classical methods are simple and offer bad to medium performance with a huge computation load. In this chapter, the classical methods that are based on simple beamforming method are discussed in detail that serves as an important background for the proposed method listed thereafter.
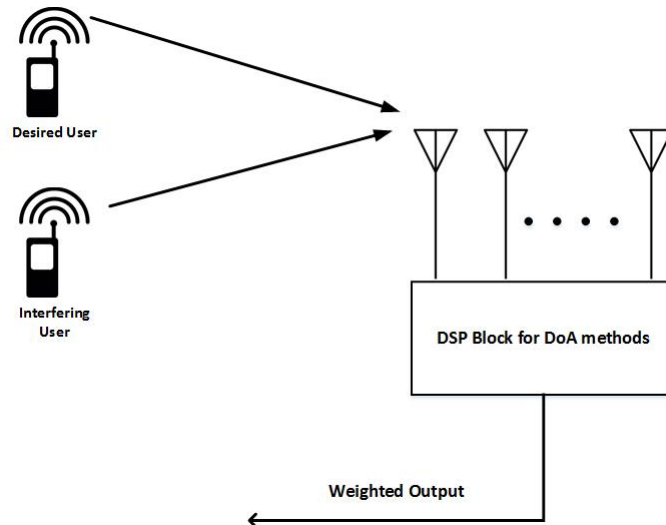
FIGURE 2.1: Antenna array processing for SoI and NSoI

The two main classical techniques for DoA estimation are *delay-and-sum* method and the minimum variance distortionless response (MVDR) method [4]. The main idea behind the classical methods is to scan a beam through space and measure the power received in each direction. However, before formulating these methods, lets describe the system parameters accordingly.

2.2 Propagation Delay in Uniform Linear Arrays

Consider an uniform linear array geometry with N elements with index numbered as $0, 1, 2, 3...., N-1$. The array elements are considered to have $\lambda/2$ (half wavelength) spacing so as to bear minimum effects of mutual coupling. Since the array elements are closely spaced, it is assumed that the signals received by the different antenna elements are correlated. The baseband signal $s(t)$ is received on the array and it's assumed that the phase of $s(t)$ received at antenna element 0 is zero. By assuming so, the phase of the other elements is calculated relative to the element 0. This is represented in Figure 2.2. Now, the time delay of arrival for the signal vector is:

$$\Delta t_k = \frac{kd \sin \theta}{c} \tag{2.2.1}$$

where c is the speed of the light.
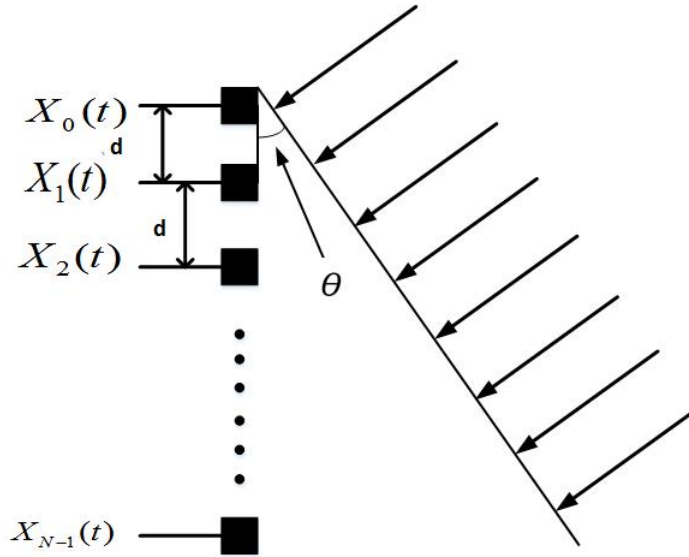
FIGURE 2.2: Plane wave received at ULA

Suppose $s(t)$ (narrowband digitally modulated signal) and its lowpass equivalent $s-l(t)$, carrier frequency f_c, and symbol period T. Then, $s(t)$ is:

$$s(t) = \text{Re}\left\{ s_l(t)e^{j2\pi f_c t} \right\} \tag{2.2.2}$$

The signal at k-th element is then:

$$x_k(t) = \text{Re}\left\{ s_l(t - \Delta t_k)e^{j2\pi f_c(t - \Delta t_k)} \right\} \tag{2.2.3}$$

If the signal $x_k(t)$ is then downconverted to baseband, the received signal in that case would be:

$$x_k(t) = s_l(t - \Delta t_k)e^{-j2\pi f_c t \Delta t_k} \tag{2.2.4}$$

2.3   Narrowband Approximation

The received baseband signal, when sampled with a sampling period of T seconds can be further represented as:

$$x_k(nT) = s_l(nT - \Delta t_k)e^{-j2\pi f_c t \Delta t_k} \tag{2.3.1}$$

In wireless digital communication, $T >> \Delta t_k, \quad k = 0, 1, 2....N - 1$, that is the symbol period is much greater than each of the propagation delay. Therefore, the following approximation can be made [7].

$$x_k(nT) \approx s_l(nT)e^{-j2\pi f_c t \Delta t_k} \tag{2.3.2}$$

The element spacing is computed with respect to wavelength as $d = D/\lambda$ and also f_c is related to λ as $c = \lambda f_c$. Using these, the equation 2.3.2 can be written as:

$$x_k(nT) \approx s_l(nT)e^{-j2\pi n d \sin\theta} \tag{2.3.3}$$

To avoid aliasing in space the distance between elements d has to be $\lambda/2$ or less [8]. This will further simplify the equation 2.3.3 to

$$x_k(nT) \approx s_l(nT)e^{-j\pi k \sin\theta} \tag{2.3.4}$$

In discrete time notation, sampled signal at the k-th element equation can be expressed as

$$x_k[n] \approx \sum_{i=0}^{r-1} s_i[n]a(\theta_i) \tag{2.3.5}$$

where r is the total signals present and the n-th symbol of the i-th signal is denoted by $s_i[n]$ for $i = 0, 1, 2....r - 1$.

2.4 Matrix Representation for Array Data

In equation 2.3.5, considering all elements of the array, i.e., $k = 0, 1, 2, ..., N-1$ in matrix form is as follows

$$
\begin{bmatrix} x_0[n] \\ x_1[n] \\ . \\ . \\ x_{N-1}[n] \end{bmatrix} = \begin{bmatrix} a_0(\theta_0) & a_0(\theta_1) & . & . & a_0(\theta_{r-1}) \\ a_1(\theta_0) & a_1(\theta_1) & . & . & a_1(\theta_{r-1}) \\ . & & . & . & . \\ . & & . & . & . \\ a_{N-1}(\theta_0) & a_{N-1}(\theta_1) & . & . & a_{N-1}(\theta_{r-1}) \end{bmatrix} \begin{bmatrix} s_0[n] \\ s_1[n] \\ . \\ . \\ s_{r-1}[n] \end{bmatrix} + \begin{bmatrix} w_0[n] \\ w_1[n] \\ . \\ . \\ w_{N-1}[n] \end{bmatrix}
$$

(2.4.1)

where $w_k[n]$ is the AWGN assumed at each element. The $N \times 1$ vector $\boldsymbol{x}_n$, the $N \times r$ matrix $\mathbf{A}$, the signal vector $\boldsymbol{s}_n$ and noise vector $\boldsymbol{w}_n$ is further represented in matrix compact form.

$$
\boldsymbol{x}_n = \begin{bmatrix} \boldsymbol{a}(\theta_0) & \boldsymbol{a}(\theta_1) & . & . & \boldsymbol{a}(\theta_{r-1}) \end{bmatrix} \boldsymbol{s}_n + \boldsymbol{w}_n = \boldsymbol{A}\boldsymbol{s}_n + \boldsymbol{w}_n
$$

(2.4.2)

The columns of matrix $\mathbf{A}$: $\boldsymbol{a}(\theta_i)$ are known as steering vectors of signal $s_i(t)$. All these steering vectors together are known as *array manifold* [9]. In some array configuration the array manifold can be found analytically but in case of complex geometry the manifold is determined practically. In this work, analytic computations for such arrays are used extensively. Since angle of arrival of each r signals is different, the columns of matrix $\mathbf{A}$ will form a linearly independent set. If there is no noise then the array output is:

$$
\boldsymbol{x}_n = \boldsymbol{A}\boldsymbol{s}_n
$$

(2.4.3)

Moreover, the received signal vector $\boldsymbol{x}_n$ is a linear combination of matrix $\mathbf{A}$ columns. Hence, these vectors span the *signal subspace*. The signal subspace idea is common to many application, for example: DoA, low rank filtering etc [9–11]. Now, antenna beamforming mechanism for classical DoA estimations will be discussed in the next section before going on to subspace based methods,

2.5   Antenna Beamforming Basics

Antenna beamforming is the process of assigning complex weights to the receive antennas so as to have a desired pattern in the direction of maximum power [12]. The weighted linear combination of the output from the array elements can be written as

$$y[n] = \sum_{k=0}^{N-1} w_k x_k[n] \tag{2.5.1}$$

where $\boldsymbol{w} \in \mathbb{C}^{N \times 1}$ (Complex weight). In vector notation:

$$y[n] = \boldsymbol{w}^H \boldsymbol{x}_n \tag{2.5.2}$$

This process of adjusting the weight vector $\boldsymbol{w}$ in such a way so that the beam is aligned towards SoI is called as beamforming or spatial filtering. There are numerous designs to compute efficient weights for a desired pattern. For a signal with an AoA as θ, the beamformer output can be given as:

$$y[k] = \frac{1}{N} \sum_{n=0}^{N-1} w_n x_n[k] = \frac{1}{N} \sum_{n=0}^{N-1} w_n s_0[k] e^{-j2\pi nd \sin \theta} = \frac{s_0[k]}{N} \sum_{n=0}^{N-1} w_n e^{-j2\pi nd \sin \theta} \tag{2.5.3}$$

The scaling factor with the signal is called the *beampattern or array factor*, which in vector notation is:

$$\boldsymbol{w}(\theta_0) = \frac{1}{N} \sum_{n=0}^{N-1} w_n e^{-jn\omega} = \boldsymbol{w}^H \boldsymbol{a}(\theta) \tag{2.5.4}$$

where $\omega = 2\pi d \sin \theta$ and $\boldsymbol{a}(\theta)$ represents the steering vector, which is given as

$$\boldsymbol{a}(\theta) = \begin{bmatrix} 1 & e^{-j\omega} & e^{-2j\omega} & . & . & e^{-j(N-1)\omega} \end{bmatrix} \tag{2.5.5}$$

2.6 Classical Methods

As the systems and beamforming basics are covered in previous sections, the two famous classical DoA estimation methods that is delay and sum method and MVDR will be discussed now in detail.

2.6.1 Delay and Sum Method

The delay-and-sum method calculates DoAs by measuring signal power at every possible angle of arrival and at the end choosing the angle that delivers maximum power [6]. The beamformer output power is given by:

$$\boldsymbol{P}(\theta) = E[\boldsymbol{y}^H\boldsymbol{y}] = E|\boldsymbol{w}^H\boldsymbol{x}_n|^2 = E|\boldsymbol{a}(\theta)^H\boldsymbol{x}_n|^2 = \boldsymbol{a}(\theta)^H\boldsymbol{R}_{xx}\boldsymbol{a}(\theta) \qquad (2.6.1)$$

When $\boldsymbol{w}$ is aligned with the steering vector of the incoming signal then $\boldsymbol{P}(\theta)$ would have peaks at those angles.

2.6.2 Capon's Minimum Variance Distortionless Response Technique

Capon's minimum variance distortionless response method (MVDR) or Minimum output energy (MoE) beamformer [13] has a different optimality criterion. The objective is to minimize output power with gain in the desired direction is kept fixed. So, any reduction in output power would be by interference suppression. The problem therefore is stated as:

$$\begin{aligned} \text{minimize} \quad & E[\boldsymbol{y}^H\boldsymbol{y}] \\ \text{subject to} \quad & \boldsymbol{w}^H\boldsymbol{a}(\theta) = 1 \end{aligned} \qquad (2.6.2)$$

The optimization problem is solved using Lagrange multiplier method that is to find minimum of $|\mathcal{L}(w;\lambda)|$. As it is know, $\boldsymbol{y} = \boldsymbol{w}^H\boldsymbol{s}[k]\boldsymbol{a}(\theta)$. Therefore, $\boldsymbol{y}^H\boldsymbol{y}$:

$$\begin{aligned} \boldsymbol{y}^H\boldsymbol{y} &= (\boldsymbol{a}(\theta)^H\boldsymbol{w}\boldsymbol{s}[k]^H) \cdot (\boldsymbol{s}[k]\boldsymbol{w}^H\boldsymbol{a}(\theta)) \\ &= \boldsymbol{a}^H\boldsymbol{w}\boldsymbol{R}_{xx}\boldsymbol{w}^H\boldsymbol{a}(\theta) \end{aligned} \qquad (2.6.3)$$

The $\mathcal{L}(w; \lambda)$ is given by:

$$\mathcal{L}(w; \lambda) = \boldsymbol{a}(\theta)^H \boldsymbol{w} \boldsymbol{R}_{xx} \boldsymbol{w}^H \boldsymbol{a}(\theta) - \lambda(\boldsymbol{w}^H \boldsymbol{a}(\theta) - 1) \tag{2.6.4}$$

Taking derivative (with respect to $\boldsymbol{w}^H$) and setting the solution to zero.

$$\begin{aligned}
\frac{d\mathcal{L}}{dw^H} &= \boldsymbol{a}(\theta)^H \boldsymbol{w} \boldsymbol{R}_{xx} \boldsymbol{a}(\theta) - \lambda \boldsymbol{a}(\theta) = 0 \\
\boldsymbol{a}(\theta)^H \boldsymbol{w} \boldsymbol{R}_{xx} \boldsymbol{a}(\theta) &= \lambda \boldsymbol{a}(\theta) \\
\boldsymbol{w} \boldsymbol{R}_{xx} &= \lambda \boldsymbol{a}(\theta) \\
\boldsymbol{w} &= \lambda \boldsymbol{R}_{xx}^{-1} \boldsymbol{a}(\theta)
\end{aligned} \tag{2.6.5}$$

Then, to find λ, substitute $\boldsymbol{w}$ to the constraint equation which results to

$$\begin{aligned}
\lambda \boldsymbol{R}_{xx}^{-1} \boldsymbol{a}(\theta)^H \boldsymbol{a}(\theta) &= 1 \\
\lambda &= \frac{1}{\boldsymbol{a}(\theta)^H \boldsymbol{R}_{xx}^{-1} \boldsymbol{a}(\theta)}
\end{aligned} \tag{2.6.6}$$

Hence, the weights of MVDR [5, 14] are given by

$$\boldsymbol{w} = \frac{\boldsymbol{R}_{xx}^{-1} \boldsymbol{a}(\theta)}{\boldsymbol{a}(\theta)^H \boldsymbol{R}_{xx}^{-1} \boldsymbol{a}(\theta)} \tag{2.6.7}$$

In summary, classical beamforming method relies on the principal of choosing DoAs along the direction from which it receives the high power. The difference between the two classical methods is in the formulation of constraint part, for example, in MVDR method, interference suppression is the constraint that the method tries to achieve apart from finding the DoAs. The next chapter will give an insight into another method of finding DoAs that is subspace based methods for DoA estimation in antenna arrays.

Chapter 3

DoA Estimation by Subspace Methods in Massive MIMO

3.1 Introduction

The subspace methods of DoA estimation for antenna arrays are based on segregating the signal and noise subspaces and utilizing these subspaces to determine the power spectrum. These methods originated from spectral estimation research [10], where the main feature is to calculate the autocorrelation or autocovariance matrix of signal with noise and then utilize eigen value decomposition to find signal and noise subspaces. The advantage of subspace methods is that they have high resolution capabilities, low complexity and are well implementable in practice.

3.2 Multiple Signal Classification Algorithm or MUSIC

The MUSIC algorithm proposed by Schmidt [11] is one of the most famous methods for DoA estimation. The method works as follows. Consider the antenna array output, which in vector form $(\boldsymbol{x}_n)$ is given as

$$\boldsymbol{x}_n = \boldsymbol{A}\boldsymbol{s}_n + \boldsymbol{w}_n \qquad (3.2.1)$$

It is assumed that $\boldsymbol{s}_n$ and $\boldsymbol{w}_n$ to be uncorrelated. The noise vector $\boldsymbol{w}_n$ is AWGN (zero mean) and correlation matrix of $\sigma^2 \boldsymbol{I}$. Defining $\boldsymbol{R}_{ss} = E[\boldsymbol{S}_n \boldsymbol{S}_n^H]$. The spatial covariance matrix is then:

$$
\begin{aligned}
\boldsymbol{R}_{xx} &= E[\boldsymbol{x}\boldsymbol{x}^H] \\
&= E[(\boldsymbol{A}\boldsymbol{S_n} + \boldsymbol{w_n})(\boldsymbol{A}\boldsymbol{S_n} + \boldsymbol{w_n})^H] \\
&= \boldsymbol{A}E[\boldsymbol{S_n}\boldsymbol{S_n}^H]\boldsymbol{A}^H + E[\boldsymbol{w_n}\boldsymbol{w_n}^H] \\
&= \boldsymbol{A}\boldsymbol{R}_{ss}\boldsymbol{A}^H + \sigma^2 \boldsymbol{I}_{N \times N} \\
&= \tilde{\boldsymbol{R}}_s + \sigma^2 \boldsymbol{I}_{N \times N}
\end{aligned}
\tag{3.2.2}
$$

$\tilde{\boldsymbol{R}}_s$: $N \times N$ matrix is the signal covariance matrix and has rank M. Therefore, $N - M$ eigenvectors belong to zero eigenvalue. Let $\boldsymbol{q}_m$ be one of those $N - M$ eigen vector. Then,

$$
\begin{aligned}
\tilde{\boldsymbol{R}}_s \boldsymbol{q}_m &= \boldsymbol{A}\boldsymbol{R}_{ss}\boldsymbol{A}^H \boldsymbol{q}_m = 0 \\
\implies \boldsymbol{A}^H \boldsymbol{q}_m &= 0
\end{aligned}
\tag{3.2.3}
$$

From equation 3.2.3, it is clear that $N - M$ eigenvectors ($\boldsymbol{q}_m$) of $\tilde{\boldsymbol{R}}_s$ are zero eigenvalue which are orthogonal to M steering vectors. This is the fundamental idea behind the basics of MUSIC. Defining $\boldsymbol{Q}_n$: $N \times (N - M)$ matrix with these eigen vectors. The *pseudo-spectrum* function plotted by MUSIC is then written as

$$
\boldsymbol{P}_{MUSIC}(\theta) = \frac{1}{\boldsymbol{a}(\theta)^H \boldsymbol{Q}_n \boldsymbol{Q}_n^H \boldsymbol{a}(\theta)}
\tag{3.2.4}
$$

In practice, the covariance matrix $\boldsymbol{R}_{xx}$ is unknown and does require taking average over many data snapshots. That is

$$
\boldsymbol{R}_{xx} = \frac{1}{K} \sum_{k=1}^{K} \boldsymbol{x}_k \boldsymbol{x}_k^H
\tag{3.2.5}
$$

where x_k is the k-th snapshot. In [15], the author has shown that $K > 2N$, for SNR $\leq$ 3 dB of the calculated optimum value.

3.3   Root MUSIC

Root music [16] is another form of MUSIC algorithm that is only applicable to uniform arrays. It provides better resolution relative to MUSIC especially at low SNR. The steering vector is then:

$$\boldsymbol{a}_n(\theta) = exp(j2\pi nd\sin(\theta)), \quad n = 0,\ 1,\ 2, ...,\ N-1, \tag{3.3.1}$$

where element spacing d is in λ's and θ is the DoA. The MUSIC spectrum as defined by equation 3.2.4 is :

$$\boldsymbol{P}_{MUSIC}(\theta) = \frac{1}{\boldsymbol{a}(\theta)^H \boldsymbol{Q}_n \boldsymbol{Q}_n^H \boldsymbol{a}(\theta)} = \frac{1}{\boldsymbol{a}(\theta)^H \boldsymbol{C} \boldsymbol{a}(\theta)} \tag{3.3.2}$$

where $\boldsymbol{C}$ is

$$\boldsymbol{C} = \boldsymbol{Q}_n \boldsymbol{Q}_n{}^H \tag{3.3.3}$$

Writing denominator as a double summation [6], that is

$$\boldsymbol{P}_{MUSIC}^{-1} = \sum_{k=0}^{N-1} \sum_{p=0}^{N-1} exp(-j2\pi pd\sin(\theta)) C_{kp} exp(j2\pi kd\sin(\theta))$$
$$\boldsymbol{P}_{MUSIC}^{-1} = \sum_{p-k=l} C_l exp(-j2\pi(p-k)d\sin(\theta)) \tag{3.3.4}$$

where, C_l is determined by the sum of the l-th diagonal of $\boldsymbol{C}$. A polynomial $D(z)$ can be defined as follows:

$$D(z) = \sum_{-N+1}^{N+1} C_l z^{-l} \tag{3.3.5}$$

The polynomial $D(z)$ is valid on the unit circle, if $\boldsymbol{P}_{MUSIC}^{-1}$ is equivalent to $D(z)$. Since in $\boldsymbol{P}_{MUSIC}$, there are r peaks but in $D(z)$ there will be r valleys or in other terms r zeros on unit circle. In absence of noise, $D(z)$ will have r zeros on unit circle, however with noise, the roots will be close to unit circle. The Root music reduces the DoA estimation to just finding roots for a $(2N+1)$ the order polynomial.

3.4 Smooth MUSIC

In a realistic wireless network situation, all the incoming signals are not uncorrelated and in these scenarios, a famous variant of MUSIC can be utilized which is known as smooth MUSIC [6]. Since the signals are correlated, the matrix $\boldsymbol{A}$ which was diagonal for music would not be the same in this case, The N array elements are divided into overlapping subarrays of size L with each having P elements. Hence, $L = N - P + 1$ that is L correlation matrices are estimated with every matrix having a dimension of $P \times P$. The smoothed correlation matrix is given as:

$$\boldsymbol{R}_L = \frac{1}{L} \sum_{l=0}^{L-1} \boldsymbol{R}_l \tag{3.4.1}$$

This formulation can detect DoA of up to $L - 1$ correlated signals.

3.5 The Minimum Norm Method

The minimum norm method [17] is a high resolution method in which a vector is defined such that it lies in the noise subspace and where the first element has the minimum norm [5, 18]. That is:

$$\boldsymbol{g} = \begin{bmatrix} 1 \\ \hat{\boldsymbol{g}} \end{bmatrix} \tag{3.5.1}$$

Once the minimum norm vector is found, DoAs are given by largest peaks of the following function [18]

$$\boldsymbol{P}_{MN}(\theta) = \frac{1}{\left| \boldsymbol{a}(\theta)^H \begin{bmatrix} 1 \\ \hat{\boldsymbol{g}} \end{bmatrix} \right|} \tag{3.5.2}$$

Let $\boldsymbol{Q}_s$ be the matrix whose columns form the signal subspace, $\boldsymbol{Q}_s$ can be partitioned as [5, 18]

$$\boldsymbol{Q}_s = \begin{bmatrix} \alpha^* \\ \bar{\boldsymbol{Q}}_s \end{bmatrix} \tag{3.5.3}$$

As vector $\boldsymbol{g}$ lies in the noise subspace, it implies:

$$\boldsymbol{Q}_s^H \begin{bmatrix} 1 \\ \hat{\boldsymbol{g}} \end{bmatrix} = 0 \tag{3.5.4}$$

The minimum frobenius norm for this equation is given by:

$$\hat{\boldsymbol{g}} = -\bar{\boldsymbol{Q}}_s (\bar{\boldsymbol{Q}}_s^H \bar{\boldsymbol{Q}}_s)^{-1} \alpha \tag{3.5.5}$$

From equation 3.5.3, it can be written as

$$I = \bar{\boldsymbol{Q}}_s (\bar{\boldsymbol{Q}}_s^H \bar{\boldsymbol{Q}}_s)^{-1} \alpha = (I - \alpha\alpha^*)^{-1} \alpha = \alpha/(1 - ||\alpha||^2) \tag{3.5.6}$$

Using equation 3.5.6, the matrix inverse calculation can be eliminated from equation 3.5.5 that is $\boldsymbol{g}$ can be obtained based on the orthonormal basis of signal subspace. This is shown as follows:

$$\hat{\boldsymbol{g}} = -\bar{\boldsymbol{Q}}_s \alpha/(1 - ||\alpha||^2) \tag{3.5.7}$$

Once $\boldsymbol{g}$ is calculated, the min-norm function is evaluated and the DoAs are found by the r peaks in the output.

3.6 Estimation of Signal Parameters via Rotational Invariance Techniques or ESPRIT

The ESPRIT method is another famous DoA estimation method that was proposed by Roy and Kailath [5, 9]. The method function as follows. Consider an array of N elements that can be further divided into $N/2$ pairs called as doublets. The displacement vector

is identical for one sensor in the doublet to its pair. The vector $\boldsymbol{x}$ and $\boldsymbol{y}$ are the data vectors corresponding to two $N/2$ element subarrays. The subarray output is then:

$$x_k[n] = \sum_{i=0}^{r-1} s_i[n] a_k(\theta_i) + w_k^{(x)}[n] \tag{3.6.1}$$

$$y_k[n] = \sum_{i=0}^{r-1} s_i[n] e^{j2\pi\Delta\sin\theta_k} a_k(\theta_i) + w_k^{(y)}[n] \tag{3.6.2}$$

where Δ is the displacement in wavelengths of the element in the doublet from its pair. The DoA estimation would be with respect to to this displacement vector. In matrix form, the output of the two subarrays $\boldsymbol{x}$ and $\boldsymbol{y}$ can be written as:

$$\boldsymbol{x}_n = \boldsymbol{A}\boldsymbol{s}_n + \boldsymbol{w}_n^{(x)} \tag{3.6.3}$$

$$\boldsymbol{y}_n = \boldsymbol{A}\boldsymbol{\Phi}\boldsymbol{s}_n + \boldsymbol{w}_n^{(y)} \tag{3.6.4}$$

where $r \times r$ diagonal matrix $\boldsymbol{\Phi}$ has diagonal elements as

$$e^{(j2\pi\Delta\sin\theta_0)}, e^{(j2\pi\Delta\sin\theta_1)}, e^{(j2\pi\Delta\sin\theta_2)}, \ldots, e^{(j2\pi\Delta\sin\theta_{r-1})}$$

A single $2N - 2$ data vector can be formed as

$$\boldsymbol{z}_n = \begin{bmatrix} \boldsymbol{X}_n \\ \boldsymbol{y}_n \end{bmatrix} = \boldsymbol{A}_b\boldsymbol{S}_n + \boldsymbol{w}_n \tag{3.6.5}$$

$$\boldsymbol{A}_b = \begin{bmatrix} \boldsymbol{A} \\ \boldsymbol{A}\boldsymbol{\Phi} \end{bmatrix}, \boldsymbol{w}_n = \begin{bmatrix} \boldsymbol{w}_n^{(x)} \\ \boldsymbol{w}_n^{(y)} \end{bmatrix} \tag{3.6.6}$$

The columns of $\boldsymbol{A}_b$ span the signal subspace and if $\boldsymbol{V}_s$ is a matrix whose columns are a basis for signal subspace corresponding to data vector $\boldsymbol{z}_n$. Then $\boldsymbol{A}_b$ and $\boldsymbol{V}_s$ can be related by a $r \times r$ transformation matrix $\boldsymbol{T}$ that is given by:

$$\boldsymbol{V}_s = \boldsymbol{A}_b T \tag{3.6.7}$$

This can be partitioned as follows:

$$\boldsymbol{V}_s = \begin{bmatrix} \boldsymbol{E}_x \\ \boldsymbol{E}_y \end{bmatrix} = \begin{bmatrix} \boldsymbol{AT} \\ \boldsymbol{A\Phi T} \end{bmatrix} \tag{3.6.8}$$

From equation 3.6.8, it can be observed that the range and space spanned by $\boldsymbol{E}_x, \boldsymbol{E}_y$ and $\boldsymbol{A}$ is same. Defining another rank r matrix $\boldsymbol{E}_{xy}$ as:

$$\boldsymbol{E}_{xy} = [\boldsymbol{E}_x \boldsymbol{E}_y] \tag{3.6.9}$$

Also, defining another matrix $\boldsymbol{F}$ of rank r with dimension of $r \times 2r$ that spans the null space of $\boldsymbol{E}_{xy}$. Therefore,

$$\boldsymbol{0} = [\boldsymbol{E}_x \boldsymbol{E}_y]\boldsymbol{F} = \boldsymbol{E}_x \boldsymbol{F}_x + \boldsymbol{E}_y \boldsymbol{F}_x = \boldsymbol{AT}\boldsymbol{F}_x + \boldsymbol{A\Phi T}\boldsymbol{F}_y \tag{3.6.10}$$

Defining $\boldsymbol{\Psi}$ as:

$$\boldsymbol{\Psi} = -\boldsymbol{F}_x[\boldsymbol{F}_y]^{-1} \tag{3.6.11}$$

Rearranging equation 3.6.10 gives :

$$\boldsymbol{E}_x \boldsymbol{\Psi} = \boldsymbol{E}_y \tag{3.6.12}$$

substituting equation 3.6.8 into equation 3.6.12, that is

$$\boldsymbol{AT\Psi} = \boldsymbol{A\Phi T} \implies \boldsymbol{AT\Psi T}^{-1} = \boldsymbol{A\Phi} \implies \boldsymbol{T\Psi T}^{-1} = \boldsymbol{\Phi} \tag{3.6.13}$$

Hence the diagonal elements of $\boldsymbol{\Phi}$ are equal to eigenvalues of $\boldsymbol{\Psi}$. So, once the eigenvalues: λ's of matrix $\boldsymbol{\Phi}$ has been computed, DoAs can be obtained as follows [9]:

$$\lambda_k = e^{j2\Delta sin\theta_k} \tag{3.6.14}$$

$$\theta_k = \arcsin\left(\frac{\arg(\lambda_k)}{2\pi\Delta}\right) \tag{3.6.15}$$
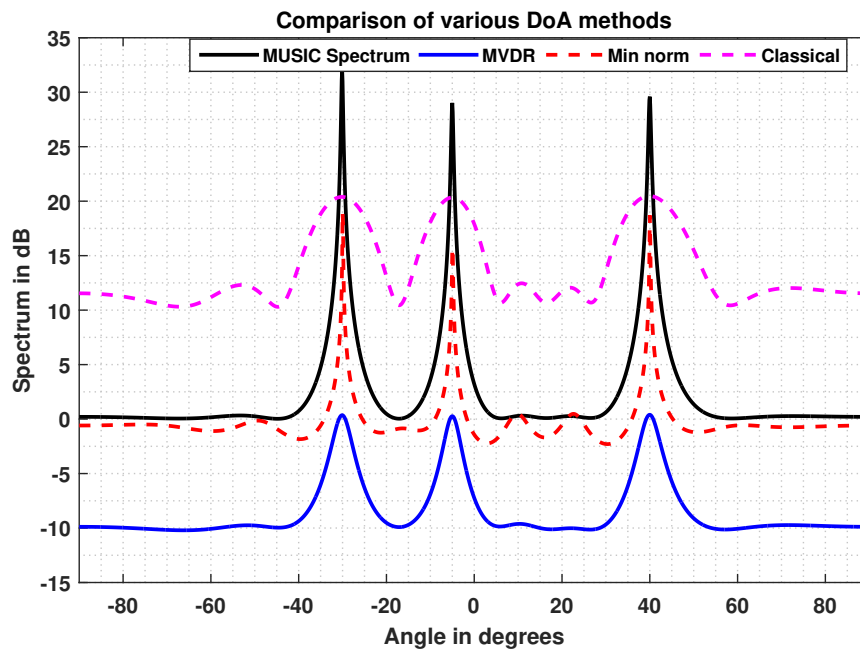
FIGURE 3.1: Comparison of various DoA methods

3.7 Simulation Results

The simulation results are plotted respectively in Figure 3.1. It is very clear that the min norm and MUSIC algorithm generate better resolution as compared to the MVDR and classical beamformer. Moreover, the output power of min norm, MUSIC algorithm and classical beamformer is higher than the MVDR. However, the main focus of these methods is to obtain high resolution DoA estimate rather than concentrate on output power, which can be managed by attenuators or by compressive sensing methods. Hence, MUSIC and min norm are the best DoA estimation methods than the other methods taken in consideration. Till now, the mutual coupling effect was not considered in the estimation methods. In the coming chapter, firstly the mutual coupling theory will be discussed in detail and then it's effect on DoA estimation will be analyzed considering various famous DoA estimation methods. Also, DoA resolution improvement and a new DoA estimation with unknown mutual coupling based on joint iterative optimization is proposed and discussed in details.

Chapter 4

Joint DoA Estimation with Mutual Coupling in Massive MIMO

4.1 Introduction

The mutual coupling estimation problem given various uncertainty in the environment such as thermal effects and aging has been a topic of interest for long [7, 19, 20]. In this chapter, first the fundamentals of mutual coupling will be discussed in brief and towards the end, a joint iterative subspace optimization with rank reduction to estimate DoAs with this dynamic unknown mutual coupling in massive MIMO networks will be proposed and discussed with its advantages.

4.2 Mutual Coupling in Antenna Array

Mutual coupling is defined as an electromagnetic interaction between array elements [21]. It affects the antenna array mainly in three ways: first is the change in the array radiation pattern, second is the change in the array manifold, and last is the change in the matching characteristic of the antenna elements [7, 19].

Consider N antenna elements of a receiver. The mutual impedance between the i-th $(i = 1, 2, 3, ..., N)$ and j-th element $(j = 1, 2, 3, ..., N)$ is formulated as:

$$Z_{ij} = \frac{V_i}{I_j} \tag{4.2.1}$$

When $i = j$, Z_{ij} is called as self impedance and if $i \neq j$, Z_{ij} is the mutual impedance. Also, V_i is the voltage on i element's open-circuited port because of current I_j of element j's port with other ports being open-circuited. Coupling matrix: $\boldsymbol{Z}$ is thus given as:

$$\boldsymbol{Z} = \begin{bmatrix} Z_{11} & Z_{12} & . & . & Z_{1N} \\ Z_{21} & Z_{22} & . & . & Z_{2N} \\ . & . & . & . & . \\ . & . & . & . & . \\ Z_{N1} & Z_{N2} & . & . & Z_{NN} \end{bmatrix} \tag{4.2.2}$$

An example of two antenna system, their self and mutual coupling parameters are depicted in Figure 4.1.
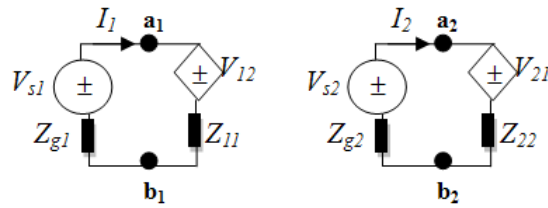
V_{s1}, V_{s2} = Excitation voltage source
Z_{g1}, Z_{g2} = Source internal impedance
Z_{11}, Z_{22} = Antenna self-impedance
I_1, I_2 = Terminal current
V_{12}, V_{21} = Coupled voltage

FIGURE 4.1: Self and mutual impedance [2]

$\boldsymbol{Z}$, when scattering matrix $\boldsymbol{S}$ is with terminating load of $Z_0 = 50 \ \Omega$ is :

$$\boldsymbol{Z} = Z_0(\boldsymbol{I}_N + \boldsymbol{S})(\boldsymbol{I}_N - \boldsymbol{S})^{-1} \tag{4.2.3}$$

where $\boldsymbol{I}_N$ is the identity matrix of dimension $N \times N$. Thus,

$$\begin{bmatrix} V_1 \\ V_2 \\ . \\ . \\ V_N \end{bmatrix} = \begin{bmatrix} Z_{11} & Z_{12} & . & . & Z_{1N} \\ Z_{21} & Z_{22} & . & . & Z_{2N} \\ . & . & . & . & . \\ . & . & . & . & . \\ Z_{N1} & Z_{N2} & . & . & Z_{NN} \end{bmatrix} \begin{bmatrix} I_1 \\ I_2 \\ . \\ . \\ I_N \end{bmatrix} \tag{4.2.4}$$

The excitation currents for the array radiation pattern to be in a required direction is :

$$\begin{bmatrix} I_1 \\ I_2 \\ . \\ . \\ I_N \end{bmatrix} = \begin{bmatrix} e^{-j\frac{2\pi}{\lambda}[\sin\theta_0(x_1\cos\phi_0 + y_1\sin\phi_0) + z_1\cos\theta_0]} \\ e^{-j\frac{2\pi}{\lambda}[\sin\theta_0(x_2\cos\phi_0 + y_2\sin\phi_0) + z_2\cos\theta_0]} \\ . \\ . \\ e^{-\frac{2\pi}{\lambda}[\sin\theta_0(x_N\cos\phi_0 + y_N\sin\phi_0) + z_N\cos\theta_0]} \end{bmatrix} \tag{4.2.5}$$

where (x_i, y_i, z_i) represent coordinates of the antenna element i. ϕ_0 and θ_0 are the DoAs (azimuth and elevation angles). The port i's driving impedance is then:

$$Z_{D_i} = \frac{V_i}{I_i} \tag{4.2.6}$$

On expansion

$$Z_{D_i} = \frac{V_i}{I_i} = \sum_{j=1}^{N} Z_{ij}\frac{I_j}{I_i} = \sum_{j=1}^{N} Z_{ij}e^{-j\frac{2\pi}{\lambda}\{\sin\theta_0[(x_i-x_j)\cos\phi_0 + (y_i-y_j)\sin\phi_0] + (z_i-z_j)\cos\theta_0\}} \tag{4.2.7}$$

Also, from circuit theory [21, 22]:

$$\begin{aligned} \boldsymbol{I} &= (\boldsymbol{Z}_g + \boldsymbol{Z})^{-1}\boldsymbol{V}_{tx} \\ \boldsymbol{v} &= \boldsymbol{Z}\boldsymbol{I} = \boldsymbol{Z}(\boldsymbol{Z}_g + \boldsymbol{Z})^{-1}\boldsymbol{V}_{tx} \end{aligned} \tag{4.2.8}$$

The circuit level model is short sighted when it comes to excitation by electromagnetic fields. Also, the radiation pattern analysis method is only accurate in directions relative to antenna system and it does require some form of interpolation [7, 23, 24] that are to

be employed to estimate the radiation patterns. However, it requires a large memory for good angular resolution. On the contrary, analysis methods minimize memory needs and hence, they are mainly employed in receiver systems [23, 25]. The main idea is that the port voltages and incident signals share a mathematical relationship:

$$\boldsymbol{v}_{rx}(\phi, \theta) = \boldsymbol{C} \boldsymbol{v}_{ideal}(\phi, \theta) \tag{4.2.9}$$

where

$$\boldsymbol{C} = \begin{bmatrix} C_{11} & C_{12} & . & . & C_{1N} \\ C_{21} & C_{22} & . & . & C_{2N} \\ . & . & . & . & . \\ . & . & . & . & . \\ C_{N1} & C_{N2} & . & . & C_{NN} \end{bmatrix} \tag{4.2.10}$$

$$\boldsymbol{v}_{ideal}(\phi, \theta) = \begin{bmatrix} e^{-j\frac{2\pi}{\lambda}[\sin\theta_0(x_1\cos\phi_0 + y_1\sin\phi_0) + z_1\cos\theta_0]} \\ e^{-j\frac{2\pi}{\lambda}[\sin\theta_0(x_2\cos\phi_0 + y_2\sin\phi_0) + z_2\cos\theta_0]} \\ . \\ . \\ e^{-\frac{2\pi}{\lambda}[\sin\theta_0(x_N\cos\phi_0 + y_N\sin\phi_0) + z_N\cos\theta_0]} \end{bmatrix}$$

The matrix $\boldsymbol{C}$ is known as coupling matrix with C_{ij} as coupling parameters between elements i and j.

4.3 Mutual Coupling Matrices for Different Arrays

Representing mutual coupling as a matrix has the biggest advantage of symmetry and sparsity that helps to design the DoA estimation system very well. The most common array configurations are linear arrays and circular arrays [7, 19, 20].

4.3.1 Linear Arrays

Since mutual coupling coefficients are negatively related to distance between antenna elements, thus for a uniform linear array (ULA) the matrix $\boldsymbol{C}$ has a banded structure.

Also, mutual coupling between two elements that are very distant is assumed to be zero. Therefore, the matrix $\boldsymbol{C}$ has a toeplitz structure that is given as:

$$\boldsymbol{C}^{\mathrm{ULA}} = \mathrm{Toeplitz}\{[C_1, C_2, C_3, ..., C_M]\} \tag{4.3.1}$$

where M represents total number of elements.

4.3.2 Circular Arrays

Under the same premise of mutual coupling relationship with distance, in uniform circular arrays (UCA), the mutual coupling matrix exhibits circulant structure with three bands: upper hand right band, center band and lower left corner band.

$$\boldsymbol{C}^{\mathrm{UCA}} = \begin{cases} \mathrm{Toeplitz}\{[C_1, C_2, C_3, ..., C_L, C_{L-1}, ...C_2]\} & \text{M is even} \\ \mathrm{Toeplitz}\{[C_1, C_2, C_3, ..., C_L, C_L, C_{L-1}, ...C_2]\} & \text{M is odd} \end{cases} \tag{4.3.2}$$

where $L = \left\{\frac{M+2}{2}\right\}$, if M is even and $L = \left\{\frac{M+1}{2}\right\}$, if M is odd.

4.4 Direction Finding in Presence of Direction Independent Mutual Coupling

Consider the array signal model described in Chapter 2, the array output with coupling is rewritten as

$$\boldsymbol{y}(t_i) = \boldsymbol{C} \sum_{k=1}^{K} \boldsymbol{a}(\theta_k) s_k(t_i) + \boldsymbol{w}(t_i), \ \text{i=1,2,...,T} \tag{4.4.1}$$

where $\boldsymbol{C} \in \mathbb{C}^{M \times M}$ is direction independent complex mutual coupling matrix, $\boldsymbol{w}(t_i)$ is the AWGN, $s_k(t_i)$ is the complex baseband source signal and $\boldsymbol{a}(\theta_k) \in \mathbb{C}^{M \times 1}$ is the steering vector belonging to k-th source. The mutual coupling matrix has a definite structure on basis of its array configuration given by equation's (4.3.1, 4.3.2). Since the system model with coupling is well set up, DoA estimation with and without coupling will be discussed in next section where the comparisons will be drawn and discussed.

4.4.1 Comparison and Simulation of DoA Algorithms in Absence and Presence of Mutual Coupling

In the presence of mutual coupling, the columns of signal subspace will have coupling induced in the steering vector that is $\boldsymbol{Ca}(\theta)$. However, the orthogonality between signal and noise subspace will still hold for subsapce based methods. Hence, the modified DoA methods will be

$$\boldsymbol{w} = \frac{\boldsymbol{R}_{xx}^{-1}\boldsymbol{Ca}(\theta)}{\boldsymbol{a}(\theta)^H\boldsymbol{C}^H\boldsymbol{R}_{xx}^{-1}\boldsymbol{Ca}(\theta)} \tag{4.4.2}$$

From Section 3.2 of Chapter 3, MUSIC method is given as

$$\begin{aligned}
\boldsymbol{R}_{xx} &= E[\boldsymbol{x}\boldsymbol{x}^H] \\
&= E[(\boldsymbol{A}\boldsymbol{S}_n + \boldsymbol{w}_n)(\boldsymbol{A}\boldsymbol{S}_n + \boldsymbol{w}_n)^H] \\
&= \boldsymbol{A}E[\boldsymbol{S}_n\boldsymbol{S}_n^H]\boldsymbol{A}^H + E[\boldsymbol{w}_n\boldsymbol{w}_n^H] \\
&= \boldsymbol{A}\boldsymbol{R}_{ss}\boldsymbol{A}^H + \sigma^2\boldsymbol{I}_{N\times N} \\
&= \tilde{\boldsymbol{R}}_s + \sigma^2\boldsymbol{I}_{N\times N}
\end{aligned} \tag{4.4.3}$$

and

$$\boldsymbol{P}_{MUSIC}(\theta) = \frac{1}{\boldsymbol{a}(\theta)^H\boldsymbol{Q}_n\boldsymbol{Q}_n^H\boldsymbol{a}(\theta)} \tag{4.4.4}$$

With mutual coupling being present, the columns of signal subspace will have coupling induced in the steering vector that is $\boldsymbol{Ca}(\theta)$. However, the orthogonality between signal and noise subspace will still hold. Hence, the music spectrum will be

$$\boldsymbol{P}_{MUSIC}(\theta) = \frac{1}{\boldsymbol{a}(\theta)^H\boldsymbol{C}^H\boldsymbol{Q}_n\boldsymbol{Q}_n^H\boldsymbol{Ca}(\theta)} \tag{4.4.5}$$

The simulation result comparing the DoA methods with and without coupling are plotted below in Figure 4.2.
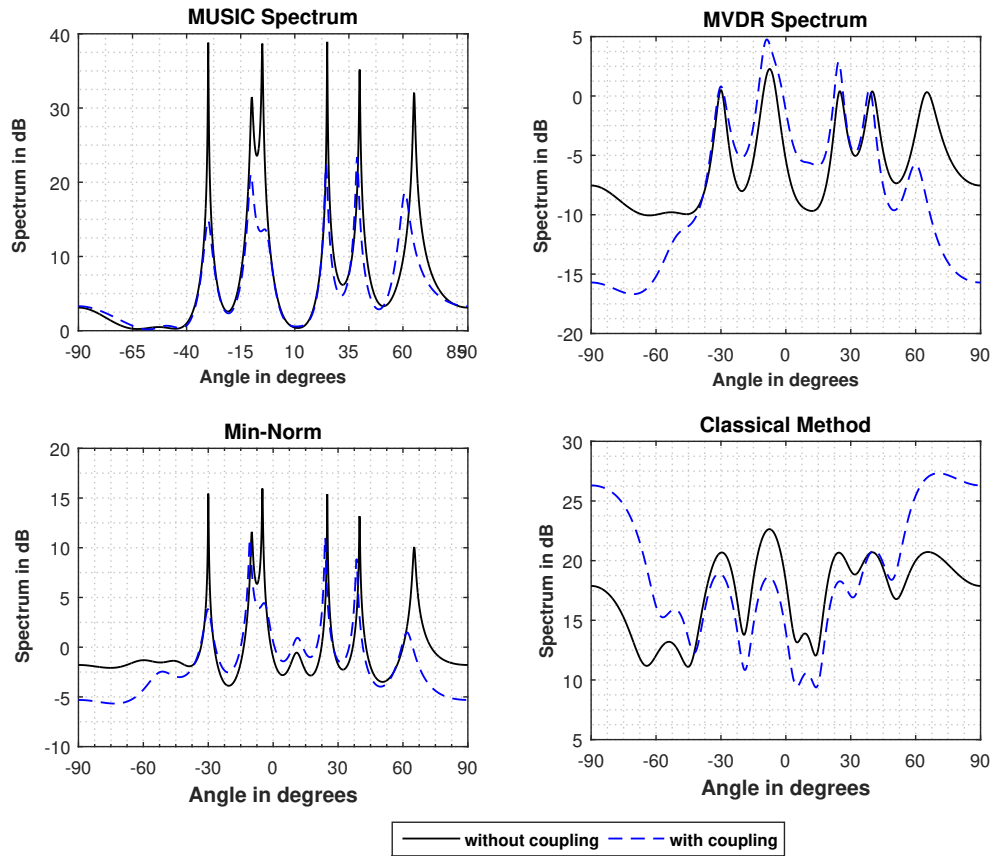
FIGURE 4.2: Comparison with and without coupling of various DoA methods

It can be easily inferred from the Figure 4.2 that the coupling changes the angular resolution by 1-4°. Considering the narrow beams in massive MIMO networks (5G), this can lead to very low SNR and thus reduction in the overall capacity. Hence, it becomes an important task to auto calibrate coupling effects.

4.5 Joint Estimation of the DOAs and Unknown Mutual Coupling Matrix

The main problem with the estimation methods is that it lacks the proper formulation of mutual coupling matrix C. Coupling matrix is a dynamic quantity which depends on many factors such as temperature, humidity etc. Therefore, it serves us a great value if it is estimated in parallel without interrupting direction finding method [7, 19, 20].

4.5.1 Algorithm for Joint Estimation of DoA and Coupling Matrix

The problem of finding DoA with unknown coupling matrix has been studied extensively in the last decade. Many algorithms have been developed depending upon the subspace methods, however their DoA resolution suffers a lot. In this section, we will utilize a simplistic data model.

The output signal vector : $\boldsymbol{x}(t)$ from an antenna array is then:

$$\boldsymbol{x}(t) = \boldsymbol{C}\boldsymbol{A}\boldsymbol{s}(t) + \boldsymbol{w}(t), \quad \boldsymbol{C} \in \mathbb{C}^{M \times M} \tag{4.5.1}$$

where

$$\boldsymbol{A} = [a(\psi_1), a(\psi_2), a(\psi_3), ..., a(\psi_N)], \quad \boldsymbol{A} \in \mathbb{C}^{M \times N} \tag{4.5.2}$$

and

$$\boldsymbol{s}(t) = [s_1(t), s_1(t), s_1(t), ..., s_1(t)]^T, \quad \boldsymbol{s}(t) \in \mathbb{C}^{N \times 1} \tag{4.5.3}$$

Due to the symmetry of the array for the cases of ULA and UCA, the unknown mutual coupling coefficients can be given by unique values : L. That is,

$$\boldsymbol{c} = [c_1, c_2, c_3, ..., c_L]^T \quad \in \mathbb{C}^{L \times 1}$$
$$1 = c1 > |c_2| > |c_3| > ..... > |c_L| > 0 \tag{4.5.4}$$

The music algorithm in Chapter 3 is re-expressed as,

$$\boldsymbol{P}_{MUSIC}(\theta) = \frac{1}{\boldsymbol{a}(\theta)^H \boldsymbol{Q}_n \boldsymbol{Q}_n^H \boldsymbol{a}(\theta)} \tag{4.5.5}$$

With unknown DoAs and mutual coupling, a cost function J is defined as:

$$J = ||\boldsymbol{Q}_n^H \boldsymbol{C}\boldsymbol{A}||_F^2 = \sum_{k=1}^{K} ||\boldsymbol{Q}_n^H \boldsymbol{C}\boldsymbol{a}(\theta_k)||^2 \tag{4.5.6}$$

Where $|| \cdot ||_F$ denotes Frobenius Norm for matrix norm and $|| \cdot ||$ denotes vector-2 norm. So, the DoA and coupling parameters is determined by minimizing J [7, 19, 20]. Taking

the advantage of the symmetry posed by ULA, matrix to vector transformation can be done, so as to make it into a QP form [7],

$$\boldsymbol{C}\boldsymbol{a}(\theta) = \boldsymbol{T}[\boldsymbol{a}(\theta)]\boldsymbol{c} \quad \in \mathbb{C}^{M \times 1} \tag{4.5.7}$$

where $\boldsymbol{c}$ is a vector referred in equation 4.5.7, and $\boldsymbol{T}[\boldsymbol{a}(\theta)] \in \mathbb{C}^{M \times L}$ is the transformation matrix whose values are determined by the corresponding array topology. Plugging equation 4.5.7 into 4.5.6, we obtain

$$J = \sum_{k=1}^{K} \boldsymbol{c}^H \boldsymbol{T}^H[\boldsymbol{a}(\theta)]\boldsymbol{Q}_n\boldsymbol{Q}_n^H\boldsymbol{T}[\boldsymbol{a}(\theta)]\boldsymbol{c} = \boldsymbol{c}^H\boldsymbol{Q}(\theta)\boldsymbol{c} \tag{4.5.8}$$

where

$$\boldsymbol{Q}(\theta) = \sum_{k=1}^{K} \boldsymbol{T}^H[\boldsymbol{a}(\theta)]\boldsymbol{Q}_n\boldsymbol{Q}_n^H\boldsymbol{T}[\boldsymbol{a}(\theta)] \tag{4.5.9}$$

As hermitian matrix $\boldsymbol{Q}(\theta)$ is independent of $\boldsymbol{c}$, J changes to a quadratic minimization problem as:

$$\min_{\{\theta_k\}_{k=1}^{K}} J = \arg\min_{\{\theta_k\}_{k=1}^{K}} \boldsymbol{c}^H\boldsymbol{Q}(\theta)\boldsymbol{c} \tag{4.5.10}$$

In general this problem has a trivial solution that is zero. So, to avoid such case, a constraint such as $||\boldsymbol{c}|| > 0$ is added to the optimization problem.

In summary, the algorithm [20] for a ULA works as follows:

Algorithm 1 An autocalibration algorithm with mutual coupling by Min Wang et al [20]

1: **Init** $\boldsymbol{c}^{(0)} = \begin{bmatrix} 1 & \frac{z_{12}}{z_{11}} \end{bmatrix}^T$ as the unique coupling matrix for ULA with the assumption that the coupling matrix is hermitian and coupling value more than half of wavelength are zero.

2: Set iteration counter to 0.

3: **Begin:** Search for K peaks using peak search method $\boldsymbol{P}(\theta) = J^{-1} = \boldsymbol{c}^H \boldsymbol{Q}(\theta) \boldsymbol{c}$ with $\boldsymbol{c}^{(0)}$. The peaks correspond to the newly estimated DoAs $\{\theta_k\}_{k=1}^K$

4: Calculate the cost function stated in equation 4.5.6

5: Perform 4.5.10 to estimate the coupling matrix with strict constraint of $\boldsymbol{c} > 0$. The result of the QP minimization gives us $\boldsymbol{c}^{(Iteration+1)}$ vector value of dimension $\mathbb{C}^{l \times 1}$

6: Normalize the $\boldsymbol{c}^{(Iteration+1)}$ with the first element of the $\boldsymbol{c}^{(Iteration+1)}$ vector

7: Substitute $\boldsymbol{c}^{(0)}$ with $\boldsymbol{c}^{(Iteration+1)}$ in the peak searching method $\boldsymbol{P}(\theta) = J^{-1} = \boldsymbol{c}^H \boldsymbol{Q}(\theta) \boldsymbol{c}$ to get new DoAs $\{\theta_k\}_{k=1}^K$

8: Increment iteration counter and go to the first step again: **Begin**.

9: **Stop** at convergence when $J^{(l-1)} - J^{(l)} \leq \delta$, where δ denotes the convergence threshold.

4.5.2 Proposed Improvement in Resolution of the DoA Estimation using Convex Optimization

Once we determined the unknown coupling matrix, we can further use L_2 *norms* and compression sensing theory to obtain a high resolution DoA spectrum [26, 27]. The goal is to construct the spectrum for DoA estimation in such a way that achieves the following.

- **Output tracking**: The new spectrum should track the original music spectrum or the reference spectrum, which as a quadratic function is given a:

$$\boldsymbol{F}_{track} = \frac{1}{\theta_I + 1} \sum_{\theta_0}^{\theta_I} (\boldsymbol{P}(\theta_i) - \boldsymbol{P}_{music}(\theta_i))^2 \quad i \in \{1, 2, ... I\} \tag{4.5.11}$$

- **Compression**: The new spectrum should not be large in magnitude. This can be written as:

$$\boldsymbol{F}_{mag} = \frac{1}{\theta_I + 1} \sum_{\theta_0}^{\theta_I} (\boldsymbol{P}(\theta_i))^2 \tag{4.5.12}$$

- **Smoothness**: The new spectrum should be as smooth as possible without spikes near the peak. Such smoothness can be mathematically written as

$$\boldsymbol{F}_{smooth} = \frac{1}{\theta_I} \sum_{\theta_0}^{\theta_{I-1}} (\boldsymbol{P}(\theta_{i+1}) - \boldsymbol{P}(\theta_i))^2 \qquad (4.5.13)$$

Finally, the function can be written as :

$$\arg \min \left(\boldsymbol{F}_{track} + \delta \boldsymbol{F}_{mag} + \eta \boldsymbol{F}_{smooth} \right) \qquad (4.5.14)$$

Where $\delta > 0$ and $\eta > 0$ are the two tuning scalars that can be used to trade off the three objectives of tracking, compression and smoothing.

4.5.3 Simulation Results

As expected the cost function converges to almost zero with every iteration and thus produces a least minimum square error as depicted in Figure 4.3.
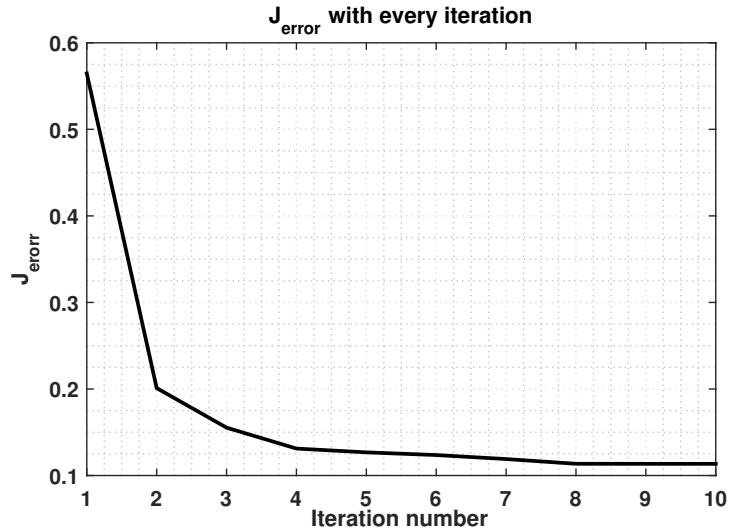

FIGURE 4.3: Cost function error every iteration.

Moreover, on performing post optimization with compressive sensing and norm optimization methods, we can further tune the output as can be seen in the Figure 4.4. Here the two plots show the tuning values as $\delta = 0$ and 0.9, while η as 0.005 and 0.9.
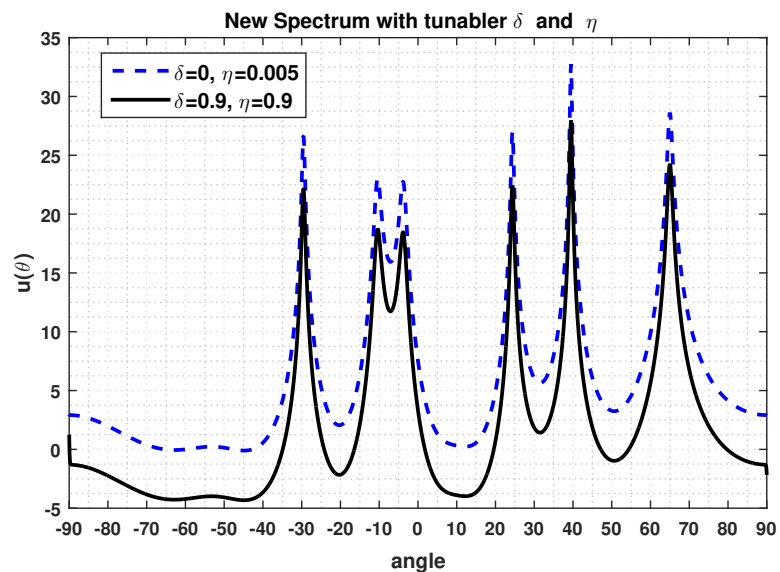

FIGURE 4.4: Result with different tunable δ and η

4.6   Joint Iterative Subspace Optimization with Rank Reduction to Estimate the DOAs and Unknown Mutual Coupling Matrix in Massive MIMO Networks

In this section, a low rank scheme known as joint iterative optimization or JIO [3] is presented for DoA estimation and then it is extended for the case of unknown coupling matrix with special emphasis towards massive MIMO networks. The rank reduction matrix changes the incoming vector into a very low dimension vector space and an secondary reduced rank vector is used to calculate DOAs. This work utilizes that rank reduced covariance matrix to calculate the cost function and thereafter estimate the unknown dynamic mutual coupling as described in the algorithm 1 of previous section. The proposed algorithm can be visualized as in Figure 4.5
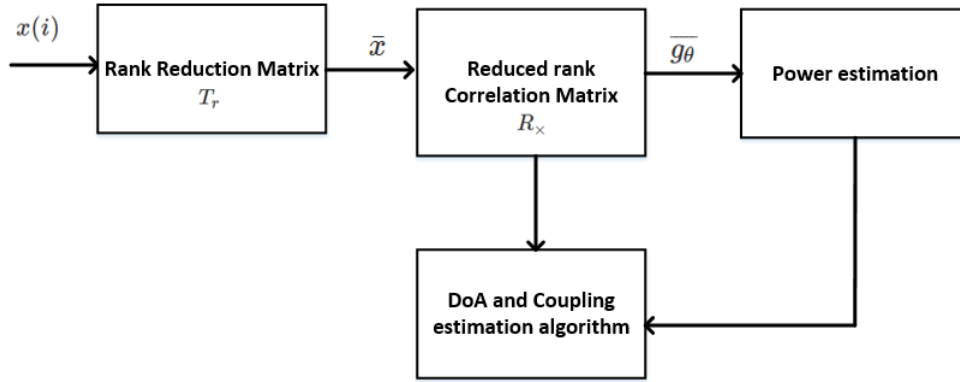
FIGURE 4.5: Proposed joint Iterative optimization method to estimate DoA and unknown coupling

4.6.1   Proposed Extended JIO

In JIO [3], a reduced rank matrix : $\boldsymbol{T}_r \in \mathbb{C}^{M \times r}$ is used to transform the input vector, $\boldsymbol{x}(i)$, to a very lower dimension that is $\boldsymbol{x} \in \mathbb{C}^{M \times 1}$ transforms to $\bar{\boldsymbol{x}} \in \mathbb{C}^{r \times 1}$, where $r << M$. The secondary reduced rank vector $\bar{\boldsymbol{g}}_\theta \in \mathbb{C}^{r \times 1}$ is used to calculate the power for the DoAs. The reduced correlation matrix is also a lower dimension space of $\hat{\bar{\boldsymbol{R}}} \in \mathbb{C}^{r \times r}$ as compared to $\hat{\boldsymbol{R}}$ which is of $\mathbb{C}^{M \times M}$ dimension. As mentioned before, the contribution of this work is to utilize the new reduced rank correlation function not just to extract DoAs but also estimate unknown mutual coupling. The main advantage of utilizing this method is the very high decrement in complexity and high ease of implementation.

The main goal therefore is to find the rank reduction matrix $\boldsymbol{T}_r$ and the secondary reduced vector $\bar{\boldsymbol{g}}_\theta$. These values are estimated with respect to θ and is formulated as an optimization problem:

$$\begin{aligned} \underset{\bar{\boldsymbol{g}}_\theta \boldsymbol{T}_r}{\text{arg minimize}} \quad & \bar{\boldsymbol{g}}_\theta^H \boldsymbol{T}_r^H \boldsymbol{R} \boldsymbol{T}_r \bar{\boldsymbol{g}}_\theta \\ \text{subject to} \quad & \bar{\boldsymbol{g}}_\theta^H \boldsymbol{T}_r^H \boldsymbol{a}(\theta) = 1 \end{aligned}$$

where $\boldsymbol{R}$ is the covariance matrix. Using lagrange multiplier, the unconstrained optimization problem is then given by:

$$\mathcal{J} = \bar{\boldsymbol{g}}_\theta^H \boldsymbol{T}_r^H \boldsymbol{R} \boldsymbol{T}_r \bar{\boldsymbol{g}}_\theta + 2\text{Real}\{\lambda[\bar{\boldsymbol{g}}_\theta^H \boldsymbol{T}_r^H \boldsymbol{a}(\theta) - 1]\} \tag{4.6.1}$$

To determine $\boldsymbol{T}_r$ and $\bar{\boldsymbol{g}}_\theta$, we assume that $\bar{\boldsymbol{g}}_\theta$ is known and then we find out $\boldsymbol{T}_r$ by exploiting the gradient of equation 4.6.1 with respect to unknown $\boldsymbol{T}_r$, that is,

$$\nabla \mathcal{J}_{T_r} = \boldsymbol{R} \boldsymbol{T}_r \bar{\boldsymbol{g}}_\theta \bar{\boldsymbol{g}}_\theta^H + \lambda_{T_r} \boldsymbol{a}(\theta) \bar{\boldsymbol{g}}_\theta^H \tag{4.6.2}$$

Equating the gradient $\nabla \mathcal{J}_{T_r}$ to zero and determining λ_{T_r}, the rank reduction matrix $\boldsymbol{T_r}$ can be expressed as

$$\boldsymbol{T}_r(i) = \frac{\hat{\boldsymbol{R}}^{-1} \boldsymbol{a}(\theta_n)}{\boldsymbol{a}^H(\theta_n) \hat{\boldsymbol{R}}^{-1} \boldsymbol{a}(\theta_n)} \frac{\bar{\boldsymbol{g}}_\theta^H(i)}{\bar{\boldsymbol{g}}_\theta(i)^2} \tag{4.6.3}$$

Similarly, taking the gradient of equation 4.6.1 with respect to unknown $\bar{\boldsymbol{g}}_\theta$, we obtain

$$\nabla \mathcal{J}_{\bar{g}_\theta} = \boldsymbol{T}_r^H \boldsymbol{R} \boldsymbol{T}_r \bar{\boldsymbol{g}}_\theta + \lambda_{\bar{g}_\theta} \boldsymbol{T}_r^H \boldsymbol{a}(\theta) \tag{4.6.4}$$

Defining reduced rank covariance matrix : $\bar{\boldsymbol{R}} = E[\bar{\boldsymbol{x}}(i)\bar{\boldsymbol{x}}^H(i)] \in \mathbb{C}^{r \times r}$ and reduced rank steering vector : $\bar{\boldsymbol{a}}(\theta) = \boldsymbol{T}_r^H \boldsymbol{a}(\theta) \in \mathbb{C}^{r \times 1}$. The final solution after determining $\lambda_{\bar{\boldsymbol{g}}_\theta}$ and equating the vector equation to zero is

$$\bar{\boldsymbol{g}}_\theta = \frac{\bar{\boldsymbol{R}}^{-1}\bar{\boldsymbol{a}}(\theta)}{\bar{\boldsymbol{a}}(\theta)^H \bar{\boldsymbol{R}}^{-1}\bar{\boldsymbol{a}}(\theta)} \tag{4.6.5}$$

From the values of reduced rank matrix $\boldsymbol{T}_r$, secondary reduced rank vector $\bar{\boldsymbol{g}}_\theta$ and reduced rank covariance matrix $\bar{\boldsymbol{R}}$, we can obtain the DoAs and mutual coupling respectively by utilizing Algorithm 1 mentioned earlier. The rank r has an impact on the resolution and has been found empirically to be in the range of $r_{min} = 3$ to $r_{max} = 7$ [3].

In summary, the proposed extended JIO algorithm can be written as follows:

Algorithm 2 Proposed algorithm

1: **Init** $\boldsymbol{T}_r(0) = [\boldsymbol{I}_{r \times r}^T \ \boldsymbol{0}_{(M-r) \times r}^T]^T$ as the reduced rank matrix.
2: **Begin**, Update for the time instance $i = 1, 2, 3, \ldots\ldots, N$
3: New input vectors: $\bar{\boldsymbol{x}}(i) = \boldsymbol{T}_r^H(i-1)\boldsymbol{x}(i)$
4: New steering vector: $\bar{\boldsymbol{a}}(\theta_n) = \boldsymbol{T}_r^H(i-1)\boldsymbol{a}(\theta_n)$
5: Recursive correlation function: $\hat{\boldsymbol{R}}(i) = \alpha\hat{\boldsymbol{R}}(i-1) + \boldsymbol{x}(i)\boldsymbol{x}^H(i)$
6: New recursive correlation function: $\hat{\bar{\boldsymbol{R}}}(i) = \alpha\hat{\bar{\boldsymbol{R}}}(i-1) + \bar{\boldsymbol{x}}(i)\bar{\boldsymbol{x}}^H(i)$
7: Update, $\bar{\boldsymbol{g}}_\theta(i) = \dfrac{\hat{\bar{\boldsymbol{R}}}(i)^{-1}\bar{\boldsymbol{a}}(\theta_n)}{\bar{\boldsymbol{a}}(\theta_n)^H \hat{\bar{\boldsymbol{R}}}(i)^{-1}\bar{\boldsymbol{a}}(\theta_n)}$
8: Update, $\boldsymbol{T}_r(i) = \dfrac{\hat{\boldsymbol{R}}^{-1}\boldsymbol{a}(\theta_n)}{\boldsymbol{a}^H(\theta_n)\hat{\boldsymbol{R}}^{-1}\boldsymbol{a}(\theta_n)} \cdot \dfrac{\bar{\boldsymbol{g}}_\theta^H(i)}{\bar{\boldsymbol{g}}_\theta(i)^2}$
9: Go to **Begin**
10: Utilize new reduced rank correlation function $\hat{\bar{\boldsymbol{R}}}(i)$ to jointly estimate the DOAs with unknown mutual coupling by applying Algorithm 1 mentioned previously. The power will be given by: $\boldsymbol{P}(\theta_n) = \dfrac{1}{\bar{\boldsymbol{a}}^H(\theta_n)\hat{\bar{\boldsymbol{R}}}(i)^{-1}\bar{\boldsymbol{a}}(\theta_n)}$

4.6.2 Simulation Results

On simulating the proposed method with rank reduction matrix of rank $r = 7$ and given DoA angles of $[0^o, 30^o, 70^o]$, the results are plotted in Figure 4.6. The covariance matrix in the proposed method is of the order of $\mathbb{C}^{7 \times 7}$ as compared to $\mathbb{C}^{100 \times 100}$ of classical or subspace based methods. Thus, the computation complexity of the proposed method is $O(M^2 + (\frac{180}{\Delta})r^2)$ or $\approx O(M^2)$ as compared to MUSIC method which is approximately $\approx O(M^3)$, where $M = 100$ and $r = 7$. Therefore, it has a great performance advantage with low computational cost over other methods in massive MIMO networks.
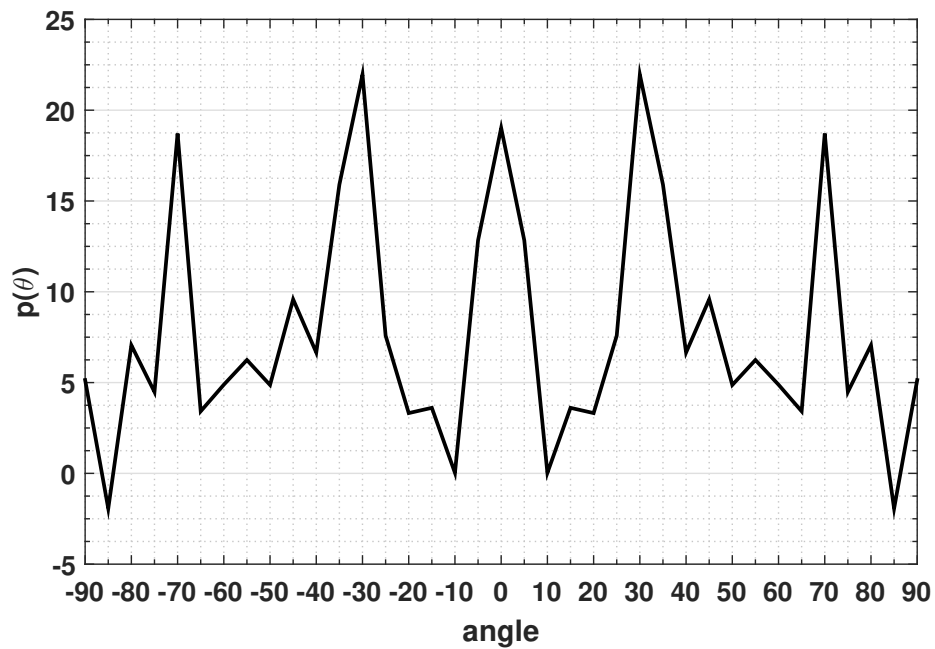

FIGURE 4.6: Joint iterative method with reduced rank optimization in massive MIMO networks

Now, the second part of the thesis about radio resource block allocation for LTE over sea will be discussed in next chapter. The advantages of the proposed method in this domain will be also highlighted.

Chapter 5

LTE Radio Resource Block Allocation Optimization in Maritime Channels

5.1 Introduction

In this chapter, the second leg of the work will be discussed and as earlier mentioned that in the absence of 5G standards, LTe was chosen to be the fit candidate. LTE networks offer diverse services that range from normal voice calls to multiple user on-line gaming. Every service that LTE offers comes with a minimum set of quality of service requirements that mainly rely on data throughput and latency. While most of the research nowadays is focused on LTE in urban landscape [28]-[30], LTE in sea environment is mostly left out. The famous urban channel models are OkumaraHata model, COST 231-Hata model, Ikegami model, or 2-Ray model. Okumara-Hata model considers open area, suburban area, and urban area for measuring path loss, while COST 231-Hata Model is just an extended part of Okumara-Hata model that considers frequencies from 1500 MHz to 2000 MHz as compared to 150 MHz to 1500 MHz. On the other hand, Ikegami Model gives deterministic prediction of field strength at specific points but underestimates loss at large distances in urban or suburban areas. In contrast, not much work has been contributed for LTE in sea environments. Only, few noted research can be found in the literature [31]-[33]. From these work, the existence of the evaporation duct

is confirmed over the sea all the time. The evaporation duct is the most dominant duct among other ducts such as surface ducts or elevated ducts in sea based environments. The main difference between the path loss propagation in sea environment and the path loss propagation in urban environment is that in sea environment, apart from direct line of sight, there are reflections from sea surface and from the evaporation duct, making it a multipath sea channel model that look like a 3-Ray path loss. Figure 5.1 shows this typical 3-Ray model.
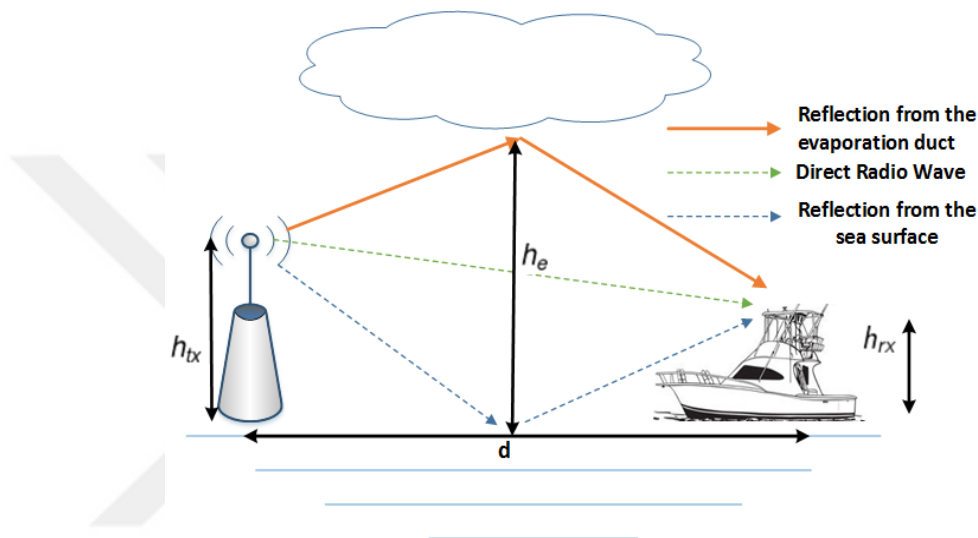

FIGURE 5.1: 3-Ray path loss model for LTE over sea, where h_{tx} is the height of the transmitter, h_{rx} is the height of receiver, h_e is the evaporation duct height and d is the distance between the transmitter and receiver.

The smallest radio resource unit in a LTE network that can be assigned to a user is called a Resource Block (RB) [34]. A resource block (RB) has 12 orthogonal frequency division multiplexing (OFDM) subcarriers that are adjacent to each other with a spacing of 15 kHz between two adjacent sub carriers. Each RB (Figure 5.2) consists of two sub-time slots of 0.5 ms and each sub-time slot utilizes 6 to 7 OFDMA symbols, depending upon whether normal cyclic prefix or extended cyclic prefix is utilized. In RB assignment, the channel state information [35] plays a vital role. Based on the CSI, an eNodeB periodically decides upon the modulation and coding scheme (MCS) [36] and assigns the number of radio blocks to its connected users. In LTE downlink, if a user has been assigned more than one RB, all these RBs have the same MCS which enhances the complexity of the radio resource allocation problem.

180 KHz (12x15 kHz) Resource Block
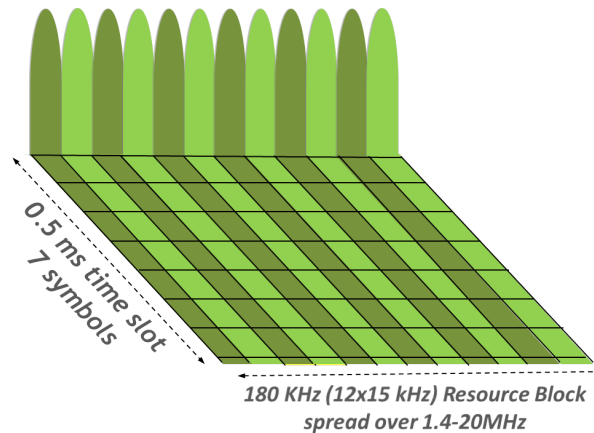spread over 1.4-20MHz

FIGURE 5.2: A radio resource block of LTE.

In this work [37], the max-min optimization technique previously used widely in wifi optimization [38, 39] is extended towards resource block allocation in marine channels. Earlier research on resource block optimization methods that use max-min technique had urban channel settings [35, 40] and therefore this much required work was undertaken.

TABLE 5.1: MCS (Modulation and Coding Schemes)

MCS	Modulation	Code Rate	SINR Threshold [dB]	Efficiency [bits/symbol]
MCS1	QPSK	1/12	-6.5	0.15
MCS2	QPSK	1/9	-4	0.23
MCS3	QPSK	1/6	-2.6	0.38
MCS4	QPSK	1/3	-1	0.60
MCS5	QPSK	1/2	1	0.88
MCS6	QPSK	3/5	3	1.18
MCS7	16QAM	1/3	6.6	1.48
MCS8	16QAM	1/2	10	1.91
MCS9	16QAM	3/5	11.4	2.41
MCS10	64QAM	1/2	11.8	2.73
MCS11	64QAM	1/2	13	3.32
MCS12	64QAM	3/5	13.8	3.90
MCS13	64QAM	3/4	15.6	4.52
MCS14	64QAM	5/6	16.8	5.12
MCS15	64QAM	11/12	17.6	5.55

5.2 LTE-SINR Path Loss Modelling in Sea Environment

In this section, path loss modelling in sea environment is considered. Equation 5.2.1, 5.2.2 and equation 5.2.3 represent the 2-ray channel, 2 ray modified channel and 3-ray channel formulation which are simulated and then plotted as seen in Figure 5.3.

$$L_{2-Ray} = -10log_{10}\left(\frac{(h_{tx} \cdot h_{rx})^2}{d^4 \cdot I}\right) \tag{5.2.1}$$

$$L_{2-RayMod.} = -10log_{10}\left(\left(\frac{\lambda}{4\pi d}\right)^2\left(2\sin\frac{2\pi h_{tx}h_{rx}}{\lambda d}\right)^2\right) \tag{5.2.2}$$

$$L_{3-Ray} = -10log_{10}\left(\left(\frac{\lambda}{4\pi d}\right)^2 \times (2(1+\triangle))^2\right) \tag{5.2.3}$$

with

$$\triangle = 2\sin\left(\frac{2\pi h_{tx}h_{rx}}{\lambda d}\right) \times \sin\left(\frac{2\pi(h_{tx}-h_e)(h_e-h_{rx})}{\lambda d}\right)$$

with the parameters being

λ : Wavelength in meters

h_{tx} : Height of transmitter in meters

h_{rx} : Height of receiver in meters

h_e : Height of evaporation duct

I : System loss parameter

d : Distance between transmitting and receiving stations.

Simulations results show that a better estimate of the received signal power in maritime channels can be acheived by 3-Ray path loss model as it gives near to practical results [33]. In the simulations, h_e is assumed to be around 25 meters and the two ferry ports selected are Uskudar and Eminonu in Istanbul, Turkey as shown on Google Maps$^{\text{TM}}$ in Figure 5.4. The distance between these two ports is around 3.7 km and the distance between two base stations on each port is around 500 meters. At any given moment, there are around 4 to 12 ships travelling from one ferry port to the other. The two lanes "Uskudar to Eminonu" and "Eminonu to Uskudar" are separated by around 300 - 400 meters. To represent ships or users, we choose equidistant points in the sea lane, and to represent eNodeBs, 4 points are fixed on the land just near to the port.
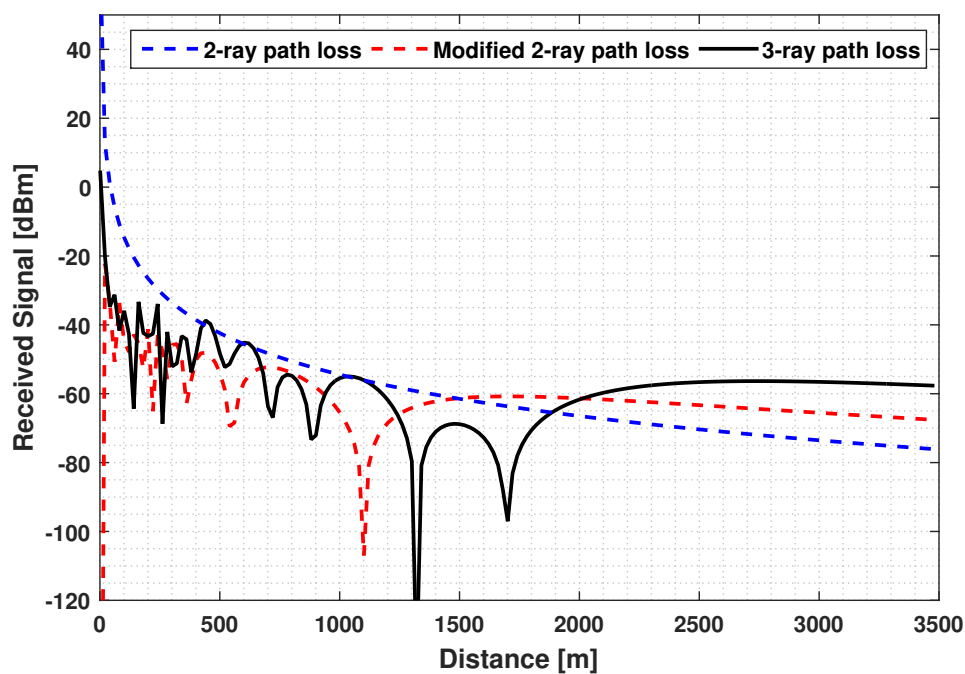
FIGURE 5.3: Simulations for different path loss models for sea channels.
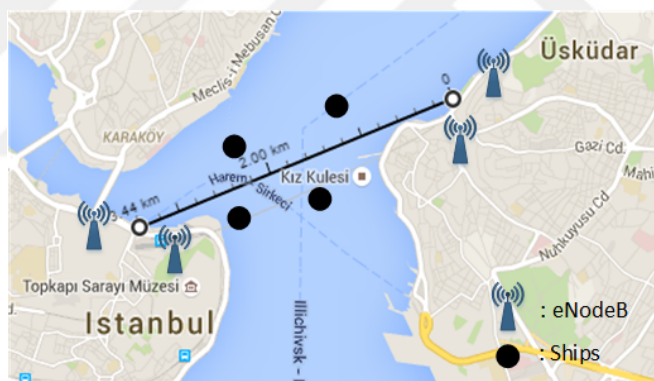
FIGURE 5.4: Eminonu and Uskudar ferry ports as seen on Google Maps$^{\text{TM}}$ with assumed ships and eNodeB positions.

5.3 LTE System Parameters and Problem Formulation

In this section, problem formulation with assumptions and the LTE system parameters required to describe the radio resource allocation problem are described out in detail.

5.3.1 Assumptions

The two main fundamental assumptions [41] regarding the detailed allocation method are: a) Throughput perceived by any user j from the connected eNodeB i depends on

number of resource block received rather than what those resources are, b) Throughput is a strictly increasing function with the increase in number of allocated resource blocks. let β_j is defined as a normalized ratio of radio resource allocated from a eNodeB i to a user j with $\beta_i \in [0,1]$, then

$$\beta_j \triangleq \frac{r_{ij}}{s_i}$$

where r_{ij} are the RB assigned to to a user j by an eNodeB i and s_i is the total available radio resources with the eNodeB i. Therefore, the throughput (T_j) as a strictly increasing function of β can be written as:

$$T_j = g_j(\beta_j).$$

These assumptions inherently take the orthogonal resource allocation and channel state information availability into picture. Intuitively, the throughput can be maximized if

$$\sum_{j=0}^{J} \beta_j = \sum_{j=0}^{J} \psi_j(T_j) = 1$$

where

$$\psi_j(T_j) \triangleq g_j^{-1}.$$

5.3.2 LTE System Parameters:

The LTE system parameters required for problem formulation are described as below:

- *user $j = 1, 2, 3, ..., J$*; a user represents a ship .

- *eNodeB $i = 1, 2, 3, ..., I$*;

- $n = 1, 2, 3, ..., N$; where n is the number of RBs.

- *SINR calculation parameters* : SINR for a user j connected to a eNodeB i is given by:

$$SINR_{i,j} = \frac{Power_{i,j} \cdot \Gamma_{i,j}}{\sum_{m=1,m\neq i}^{I} Power_{m,j} \cdot \Gamma_{m,j} + \sigma^2}$$

where $\Gamma_{i,j}$ is the channel gain between eNodeB i and user j, σ^2 is the zero mean noise variance. The formulation reflects the link conditions for the application in radio resource block allocation.

- *Throughput space matrix* : The throughput space matrix is formulated as:

$$\boldsymbol{Th}\,[I]\,[J] = \bar{T}_{ij}. \; \forall i \in [1, I], j \in [1, J]$$

The throughput space matrix entries ($\bar{T}_{ij}$'s) are defined one by one as throughput per RB between the user j and eNodeB i. The calculation is done on the mapping of MCS values to SINR levels [35, 36] as given in Table 5.1.

The demand per user is represented as :

$$D_j = \phi$$

where ϕ represents the minimum best throughput which is guaranteed to a user in the network under study.

5.3.3   Problem Formulation:

Taking all these assumptions and system parameters into consideration, problem formulation of the different radio resource allocation methods is worked out as follows

5.3.3.1   Max-min Problem Formulation

Firstly, all users are assumed to be in the transmission range of all eNodeB's and also it is assumed that the eNodeB's in the network have perfect knowledge of channel state information. The objective function of the max-min method that is maximization of the minimum throughput of the links in the network can be written as equation 5.3.1. It is further simplified in two step as equation 5.3.2 and equation 5.3.3.

$$\max_{i \in I} \min \ \arg \left(\sum_{i=1}^{I} (\bar{T}_{ij} \times K_{ij}) \right) \quad \forall \, j \in [1, J] \tag{5.3.1}$$

$$Maximize \ (\phi) \tag{5.3.2}$$

$$\sum_{i=1}^{I} \left(\bar{T}_{ij} \times K_{ij} \right) \geq \phi, \quad \forall \, j \in [1, J] \tag{5.3.3}$$

The constraint space is given by:

$$Y_{ij} \in \{0, 1\} \tag{5.3.4}$$

$$\sum_{j=1}^{J} K_{ij} \leq N, \quad \forall \, i \in [1, I] \tag{5.3.5}$$

$$\sum_{i=1}^{I} Y_{ij} = 1, \quad \forall \, j \in [1, J] \tag{5.3.6}$$

$$K_{ij} = Y_{ij} \times N, \quad \forall \, i, j \tag{5.3.7}$$

$$K_{ij} \geq (D_j / \bar{T}_{ij}) \times Y_{ij}. \quad \forall \, i, j \tag{5.3.8}$$

where Y_{ij} denotes connection between an eNodeB and a user, K_{ij} is an integer decision variable that signifies how many number of RBs can be assigned to a user j from an eNodeB i. Constraint equation (5.3.5) represents the upper cap of the RBs available at a eNodeB to be N and equation (5.3.6), $\left(\sum_{i=1}^{I} Y_{ij} \right)$ is equal to 1 for a successful connection between eNodeB i and a user j else it is zero. Furthermore, equation (5.3.7) makes sure that a user is connected to only one eNodeB that is RBs (K_{ij}) are allocated to the only defined connection (Y_{ij}). Finally, constraint equation (5.3.8) gives the relationship between capacity and demand D_j.

5.3.3.2 Round Robin Method

The round robin allocation method is formulated in such a way so that every user gets equal equal number of resource block allocation from eNodeB [41]. Hence, for a user j the throughput $\bar{T}_{ij}$ is given as :

$$\bar{T}_{ij} = \frac{\sum_{j \in J} \tilde{T}_j}{J} \quad \forall j \ \in [1, J], \tag{5.3.9}$$

where $\tilde{T}_j$ is the throughput at j^{th} user and J resents all users.

5.3.3.3 Opportunistic Method

In opportunistic case, the objective of the problem is formulated as in such a manner that each eNodeB allocates maximum RBs to a high throughput link as compared to low throughput links while assuring that every user is connected to eNodeBs. The constraint space for such maximization problem [41] will remain the same as of the max-min method described earlier.

$$
\max_{i \in I} \ \arg \left(\sum_{i=1}^{I} \left(\bar{T}_{ij} \times K_{ij} \right) \right) \quad \forall j \ \in [1, J]
$$

$$
Y_{ij} \in \{0, 1\}
$$

$$
\sum_{j=1}^{J} K_{ij} \leq N, \quad \forall \, i \in [1, I]
$$

$$
\sum_{i=1}^{I} Y_{ij} = 1, \quad \forall \, j \in [1, J]
$$

$$
K_{ij} = Y_{ij} \times N, \quad \forall \, i, j
$$

$$
K_{ij} \geq (D_j / \bar{T}_{ij}) \times Y_{ij} \quad \forall \, i, j
$$

5.3.4 Performance Comparisons

The most popular Jain index [42], [43] is used to compare these methods. The Jain index for a user j with throughput $\tilde{T}_j$ is given as:

$$
F = \frac{\left(\sum_{j \in J} \tilde{T}_j \right)^2}{N \sum_{j \in J} \tilde{T}_j^2} \quad \forall j \ \in [1, J].
$$

Table 5.2 summarizes all the LTE system parameters used in the simulations.

Parameters	Values
Carrier Frequency	2750 MHz
Number of RBs per eNodeB	25
OFDM data symbol per sub time slot	7
Antenna	2x2 MIMO
eNodeB Tx power	43 dBm
Height of Tx	20 meter
Height of Rx	3 meter
Height of Evaporation Duct	25 meter
Cable loss	3 dBm
Antenna Pattern	Omnidirectional
Carriers per RB	12
Noise Variance	1

5.4   Simulation Results

This section describes the simulation results that were done with IBM-CPLEX [44] software. The resource allocation fairness index were calculated by Jain Index and the values are listed in Table 5.3 and a sample 8 user resource allocation is listed in Table 5.4.

TABLE 5.3: Fairness index of different allocation methods with user densities

Number of Users	4	6	8	10	12
Max-Min	0.96	0.85	0.56	0.52	0.94
Opportunistic	0.56	0.37	0.39	0.25	0.26
Round Robin	0.5	0.51	0.59	0.58	0.47

TABLE 5.4: A sample 8 user resource block allocation

eNodeB index number	2	2	1	4	4	3	4	3
Connected user index number	1	2	3	4	5	6	7	8
Max-Min Method (RB's)	2	23	25	12	8	21	5	4
Round Robin Method (RB's)	13	12	25	8	8	12	9	13
Opportunistic Method (RB's)	25	1	25	1	1	1	21	25

Also, on close analysis of the simulation results with individual user densities (Figures. 5.6- 5.8), it can be safely concluded that the max-min method guarantees better minimum data throughput per user as compared to the other two methods. This is because the max-min method first allocates RBs to the worst throughput links and then to better throughput links, thus maximizing the minimum throughput of the links in the network. Moreover, the max-min method balances the overall network throughput

uniformly with increasing number of the user density than the other two optimization methods.
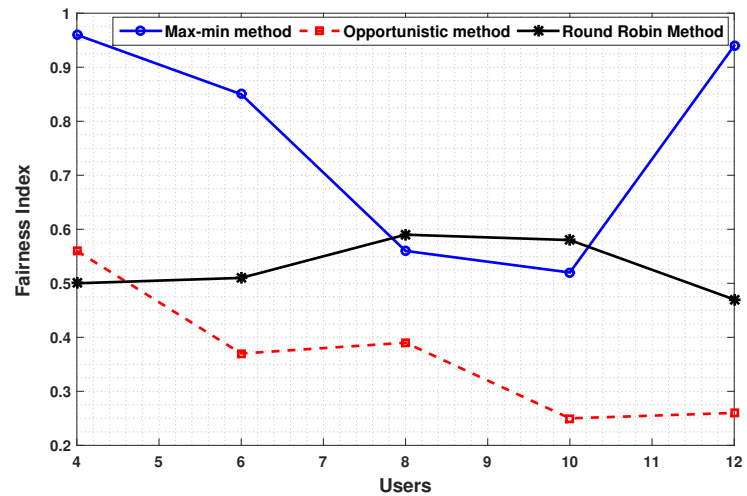

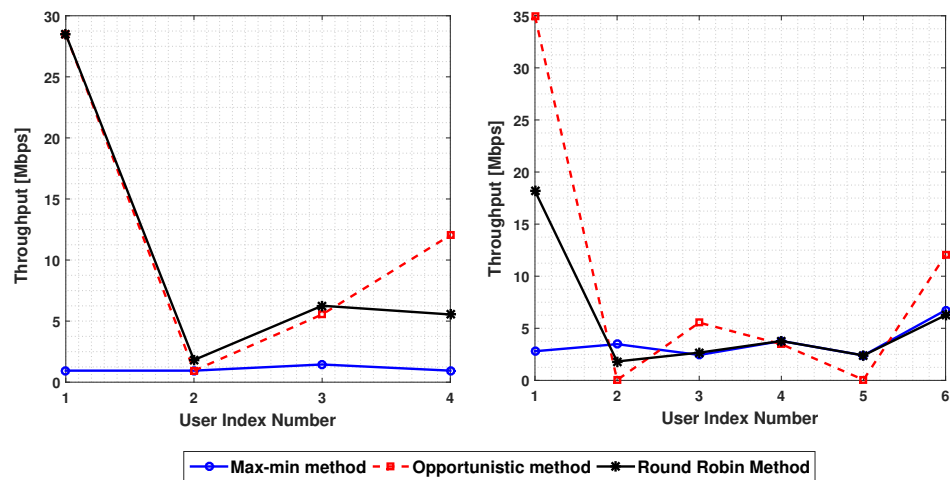FIGURE 5.5: Fairness of algorithms with user density.

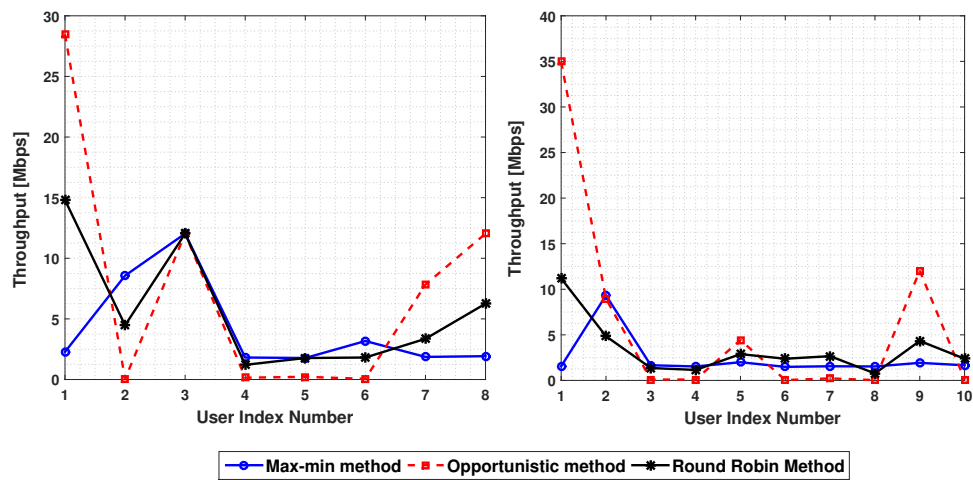FIGURE 5.6: Individual user throughput for 4 and 6 user scenarios

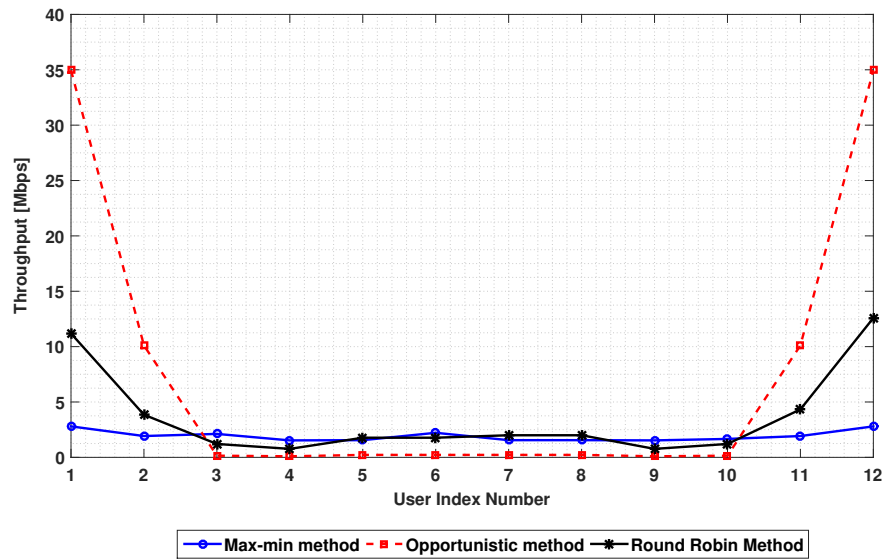FIGURE 5.7: Individual user throughput for 8 and 10 user scenarios

FIGURE 5.8: Individual user throughput for 12 user scenario

In summary, this work simulates the proper maritime channel (3-ray model) for the optimization problem and based on that describes the performance of radio resource allocation methods. It was found out that the max-min methods performs superior than round robin or opportunistic methods. Furthermore, it was also observed that with even variable user densities, the max-min optimization method performs significantly better with good fairness as compared to the opportunistic and round robin methods.

Chapter 6

Conclusion and Future Work

6.1 Conclusion

As we move towards 5G implementation, it becomes very important to study these systems inside put and work upon their limitations. One of the main goal of this work was to study and propose a low computation complexity based DoA estimation method for massive MIMO in 5G. The complete literature survey for the background on various methods were discussed in Chapter 2 and Chapter 3 with introduction to 5G in Chapter 1. This work extended the use of JIO [3] algorithm with the unique difference being that it assumes that the mutual coupling is also present and requires to be estimated. It was also shown in Chapter 4 that the computation complexity of the proposed method is $\approx O(M^2 + (\frac{180}{\Delta})r^2)$ or $\approx O(M^2)$ as compared to MUSIC which has computation complexity of the order of $\approx O(M^3)$, where $M = 100$ and $r = 7$. That is a big advantage of using joint iterative methods with rank reduction optimization in massive MIMO rather than classical or subspace based methods. Furthermore, in absence of any 5G standards, radio resource block allocation method was also studied for maritime channels considering LTE network and a max-min method was proposed in that cause in Chapter 5. The results of the proposed max-min resource allocation method reflected the superiority over other methods in terms of fairness with variable load. Mathematically speaking, the core of this thesis was based on the application of convex optimization and linear algebra theory. It included joint iterative method with reduced rank matrix optimization, quadratic programming (QP), compressed sensing, L_2 norms and max-min optimization to formulate and solve the problem in hand.

6.2   Future Work

The future work with respect to massive MIMO for 5G has immense potential and demand. One of the main idea to work upon would be to compare the results from an implemented 5G system or 5G test bed with the simulation results mentioned in this thesis. Apart from that, directional dependent mutual coupling will be an interesting field to prospect and investigate. The joint estimation of DoAs with unknown mutual coupling in carrier aggregation mode is also an open turf for research in 4G and 5G as mutual coupling will be different for different frequency bands. Antenna switching algorithm to tackle mutual coupling in massive MIMO is another open research topic. Moreover, there are some advances in antenna switching domain too, however, lack of 5G standards can be an issue with the research. Also, for the radio resource block allocation method, the joint optimization of power and frequency per sub carrier in LTE network over the sea extended to 5G networks would be yet another interesting topic. Overall, 5G is an open field of opportunities to work upon which has the bright prospects of bringing the next generation of networked society into reality.

Bibliography

[1] E. G. Larsson, O. Edfors, F. Tufvesson, and T. L. Marzetta, "Massive mimo for next generation wireless systems," *IEEE Communications Magazine*, vol. 52, no. 2, pp. 186–195, 2014.

[2] C. U. Ndujiuba, O. Oshin, and N. Nkordeh, "Mimo deficiencies due to antenna coupling," *International Journal of Networks and Communications*, vol. 5, no. 1, pp. 10–17, 2015.

[3] L. Wang, R. C. de Lamare, and M. Haardt, "Direction finding algorithms based on joint iterative subspace optimization," *IEEE Transactions on Aerospace and Electronic Systems*, vol. 50, no. 4, pp. 2541–2553, 2014.

[4] S. S. Haykin, *Adaptive filter theory*. Pearson Education India, 2008.

[5] J. Foutz, A. Spanias, and M. K. Banavar, "Narrowband direction of arrival estimation for antenna arrays," *Synthesis Lectures on Antennas*, vol. 3, no. 1, pp. 1–76, 2008.

[6] J. C. Liberti and T. S. Rappaport, *Smart antennas for wireless communications: IS-95 and third generation CDMA applications*. Prentice Hall PTR, 1999.

[7] B. Friedlander and A. J. Weiss, "Direction finding in the presence of mutual coupling," *IEEE transactions on antennas and propagation*, vol. 39, no. 3, pp. 273–284, 1991.

[8] H. Krim and M. Viberg, "Two decades of array signal processing research: the parametric approach," *IEEE signal processing magazine*, vol. 13, no. 4, pp. 67–94, 1996.

[9] R. Roy and T. Kailath, "Esprit-estimation of signal parameters via rotational invariance techniques," *IEEE Transactions on acoustics, speech, and signal processing*, vol. 37, no. 7, pp. 984–995, 1989.

[10] P. Strobach, "Fast recursive low-rank linear prediction frequency estimation algorithms," *IEEE transactions on signal processing*, vol. 44, no. 4, pp. 834–847, 1996.

[11] R. Schmidt, "Multiple emitter location and signal parameter estimation," *IEEE transactions on antennas and propagation*, vol. 34, no. 3, pp. 276–280, 1986.

[12] L. C. Godara, "Application of antenna arrays to mobile communications. ii. beamforming and direction-of-arrival considerations," *Proceedings of the IEEE*, vol. 85, no. 8, pp. 1195–1245, 1997.

[13] A. Alexiou and M. Haardt, "Smart antenna technologies for future wireless systems: trends and challenges," *IEEE Communications Magazine*, vol. 42, no. 9, pp. 90–97, 2004.

[14] J. Capon, "High-resolution frequency-wavenumber spectrum analysis," *Proceedings of the IEEE*, vol. 57, no. 8, pp. 1408–1418, 1969.

[15] I. S. Reed, J. D. Mallett, and L. E. Brennan, "Rapid convergence rate in adaptive arrays," *IEEE Transactions on Aerospace and Electronic Systems*, no. 6, pp. 853–863, 1974.

[16] A. Barabell, "Improving the resolution performance of eigenstructure-based direction-finding algorithms," in *Acoustics, Speech, and Signal Processing, IEEE International Conference on ICASSP'83.*, vol. 8.   IEEE, 1983, pp. 336–339.

[17] R. Kumaresan and D. W. Tufts, "Estimating the angles of arrival of multiple plane waves," *IEEE Transactions on Aerospace and Electronic Systems*, no. 1, pp. 134–139, 1983.

[18] P. Stoica and R. L. Moses, *Introduction to spectral analysis.*   Prentice hall Upper Saddle River, 1997, vol. 1.

[19] A. Elbir, "Direction finding in the presence of direction-dependent mutual coupling," *IEEE Antennas and Wireless Propagation Letters*, 2017.

[20] M. Wang, X. Ma, S. Yan, and C. Hao, "An autocalibration algorithm for uniform circular array with unknown mutual coupling," *IEEE Antennas and Wireless Propagation Letters*, vol. 15, pp. 12–15, 2016.

[21] C. A. Balanis, *Antenna theory: analysis and design.* John Wiley & Sons, 2016.

[22] W. L. Stutzman and G. A. Thiele, *Antenna theory and design.* John Wiley & Sons, 2012.

[23] S. Henault and Y. Antar, "Unifying the theory of mutual coupling compensation in antenna arrays," *IEEE Antennas and Propagation Magazine*, vol. 57, no. 2, pp. 104–122, 2015.

[24] R. O. Schmidt, "Multilinear array manifold interpolation," *IEEE transactions on signal processing*, vol. 40, no. 4, pp. 857–866, 1992.

[25] T. Su and H. Ling, "On modeling mutual coupling in antenna arrays using the coupling matrix," *Microwave and Optical Technology Letters*, vol. 28, no. 4, pp. 231–237, 2001.

[26] M. Grant and S. Boyd, "CVX: Matlab software for disciplined convex programming, version 2.1," http://cvxr.com/cvx, Mar. 2014.

[27] ——, "Graph implementations for nonsmooth convex programs," in *Recent Advances in Learning and Control*, ser. Lecture Notes in Control and Information Sciences, V. Blondel, S. Boyd, and H. Kimura, Eds. Springer-Verlag Limited, 2008, pp. 95–110, http://stanford.edu/~boyd/graph_dcp.html.

[28] N. Shabbir, M. T. Sadiq, H. Kashif, and R. Ullah, "Comparison of radio propagation models for long term evolution (LTE) network," *arXiv preprint arXiv:1110.1519*, 2011.

[29] Y. Ahmad, W. Hassan, T. A. Rahman *et al.*, "Studying different propagation models for LTE-A system," in *Computer and Communication Engineering (ICCCE), 2012 International Conference on.* IEEE, 2012.

[30] Y. Corre and Y. Lostanlen, "Three-dimensional urban EM wave propagation model for radio network planning and optimization over large areas," *Vehicular Technology, IEEE Transactions on*, 2009.

[31] S. D. Gunashekar, E. M. Warrington, D. R. Siddle, and P. Valtr, "Signal strength variations at 2 GHz for three sea paths in the British Channel Islands: Detailed discussion and propagation modeling," *Radio Science*, 2007.

[32] Q. Lei and M. Rice, "Multipath channel model for over-water aeronautical telemetry," *Aerospace and Electronic Systems, IEEE Transactions on*, April 2009.

[33] Y. H. Lee, F. Dong, and Y. S. Meng, "Near sea-surface mobile radiowave propagation at 5 GHz: measurements and modeling," *Radioengineering*, 2014.

[34] A. Ghosh, R. Ratasuk, B. Mondal, N. Mangalvedhe, and T. Thomas, "LTE-advanced: Next-generation wireless broadband technology," *Wireless Commun.*, 2010.

[35] D. López-Pérez, A. Ladányi, A. Jüttner, H. Rivano, and J. Zhang, "Optimization method for the joint allocation of modulation schemes, coding rates, resource blocks and power in self-organizing LTE networks," in *INFOCOM, 2011 Proceedings IEEE*. IEEE, 2011.

[36] J. Fan, Q. Yin, G. Li, B. Peng, and X. Zhu, "MCS selection for throughput improvement in downlink LTE systems," in *Computer Communications and Networks (ICCCN), 2011 Proceedings of 20th International Conference on*, July 2011.

[37] A. Kachroo, M. K. Ozdemir, and H. Tekiner-Mogulkoc, "Optimization of lte radio resource block allocation for maritime channels," in *Sarnoff Symposium, 2016 IEEE 37th*. IEEE, 2016, pp. 88–93.

[38] A. Kachroo, J. Park, and H. Kim, "Channel assignment with transmission power optimization method for high throughput in multi-access point wlan," in *Wireless Communications and Mobile Computing Conference (IWCMC), 2015 International*. IEEE, 2015, pp. 314–319.

[39] M. Pióro, M. Żotkiewicz, B. Staehle, D. Staehle, and D. Yuan, "On max–min fair flow optimization in wireless mesh networks," *Ad Hoc Networks*, vol. 13, pp. 134–152, 2014.

[40] E. Karipidis, N. Sidiropoulos, and Z.-Q. Luo, "Quality of service and max-min fair transmit beamforming to multiple cochannel multicast groups," *Signal Processing, IEEE Transactions on*, vol. 56, no. 3, March 2008.

[41] F. Zabini, A. Bazzi, and B. Masini, "Throughput versus fairness tradeoff analysis," in *Communications (ICC), 2013 IEEE international conference on*. IEEE, 2013.

[42] R. Jain, D.-M. Chiu, and W. R. Hawe, *A quantitative measure of fairness and discrimination for resource allocation in shared computer system*. Eastern Research Laboratory, Digital Equipment Corporation Hudson, MA, 1984, vol. 38.

[43] H. T. Cheng and W. Zhuang, "An optimization framework for balancing throughput and fairness in wireless networks with qos support," *Wireless Communications, IEEE Transactions on*, vol. 7, no. 2, pp. 584–593, 2008.

[44] *CPLEX*, http://www.ibm.com/software/integration/optimization/cplex/.